UNIVERSITY OF STOCKHOLM

INSTITUTE OF PHYSICS

REPORT

ISOSPIN ANALYSIS OF SINGLE ρ AND f^0 PRODUCTION IN pN COLLISIONS IN THE ENERGY RANGE 7-24 GeV

V. Bakken, T. Jacobsen, H. Johansson, P. Lundborg, J. Mäkelä, R. Møllerud, J. E. Olsson, M. Pimiä, B. Selldén and E. Sundell

USIP Report 76 - 14 April 1976

ISOSPIN ANALYSIS OF SINGLE ρ AND f^{0} PRODUCTION IN pN COLLISIONS IN THE ENERGY RANGE 7-24 GeV

V. Bakken, T. Jacobsen, H. Johansson, P. Lundborg, J. Mäkelä, R. Møllerud, J. E. Olsson, M. Pimiä, B. Selldén and E. Sundell

USIP Report 76 - 14 April 1976

ISOSPIN ANALYSIS OF SINGLE ρ AND f^0 PRODUCTION IN pN COLLISIONS IN THE ENERGY RANGE 7-24 GeV

V. Bakken[x], T. Jacobsen[x], H. Johansson[+], P. Lundborg[+], J. Mäkelä[*],
R. Møllerud[o], J.E. Olsson[x xx], M. Pimiä[*], B. Selldén[+] and
E. Sundell[ж]

ABSTRACT

New data on the ractions $pp \rightarrow pp\rho^0$, $pn \rightarrow pn\rho^0$ and $pn \rightarrow pp\rho^-$ and new data on the reactions $pp \rightarrow ppf^0$ and $pn \rightarrow ppf^0$ at 19 GeV/c are used to study the reactions $NN \rightarrow NN\rho$ and $NN \rightarrow NNf^0$ in terms of isospin amplitudes. The results are compared to the results of a previous analysis of single pion production in pN-collisions at the same energy.

Contrary to the pion case, where the isoscalar amplitude was dominating, no amplitude dominates ρ production at 19 GeV/c. Available data at other energies are used to study the energy dependence of the amplitudes.

o) The Niels Bohr Institute, University of Copenhagen
*) Department of Nuclear Physics, University of Helsinki
ж) Department of Physics, Åbo Akademi
x) Institute of Physics, University of Oslo
+) Institute of Physics, University of Stockholm
xx) Now at DESY, Hamburg

1. INTRODUCTION

One of the main interests in analysing production processes is to find out the nature of the exchange mechanism. For single particle production in high energy hadron-hadron collisions this may to some extent be done by an s-channel isospin analysis, where the isospin of the exchange is obtained. Recently such an analysis has been performed for single pion production in nucleon-nucleon (NN) collisions [1]. In this paper we study single ρ and f° production to investigate any difference in the production mechanism for single π, ρ and f production. The analysis is more difficult in the ρ and f° cases than in the pion case because of the much lower production cross sections and the problem of the non-resonant background.

In section 2 we give a short outline of the method of analysis. We will use some new data from our pd-experiment at 19 GeV/c, and some details of this experiment are given in section 3 where also the cross sections needed are evaluated. In section 4 the results of the analysis at 19 GeV/c are presented while in section 5 we use available data at other energies to obtain the energy dependence of the isospin cross sections. A discussion of the results follows in section 6.

2. METHOD OF ANALYSIS

As in single pion production three isospin amplitudes are necessary and sufficient to describe single ρ production in NN collisions. For single f^0 production two such amplitudes are sufficient. The set of amplitudes may be chosen in a variety of ways, and the different sets are equivalent and related by linear transformations.

For single pion production we used in ref. [1] a representation in which the t-channel exchange carries isospin I_x and the produced meson and one final state nucleon couple to a system with isospin I. This is a convenient choice when the secondary particles are peripherally produced as in the case of single pion production at high energy. The corresponding amplitudes get direct physical significance only when the produced meson and one of the nucleons form a physical (i.e. not only a kinematical) subsystem. Since the production of ρ and f^0 shows a peripheral structure at our energy, this representation will also be used in the present analysis. However, the degree of peripherality is somewhat difficult to ascertain because these resonances reside on a background of non-resonant events.

We will also discuss the reactions in terms of a double peripheral representation where the isospin amplitudes are specified by the isospins of the exchanges, I_1 and I_2.

2.1 $\underline{N_1N_2 \to N_3N_4\rho}$

Using the representation of fig. 1a, the symbol $M_I^{I_x}$ denotes the amplitude for t-channel exchange of isospin I_x with production of a ρ-nucleon cluster of isospin I. If charge-symmetric reactions are disregarded we have seven independent nucleon-nucleon reactions leading to the production of a ρ meson. The cross sections for these reactions are given by the isospin amplitudes according to the equations 1a-1g [2]:

$$\sigma_1 \equiv \sigma(p_1p_2 \to p_3(p_4\rho^o)) = \frac{1}{3} \int |M^0_{1/2} - \frac{1}{3} M^1_{1/2} - \frac{2}{3} M^1_{3/2}|^2 dR \tag{1a}$$

$$\sigma_2 \equiv \sigma(p_1n_2 \to p_3(p_4\rho^-)) = \frac{2}{3} \int |M^0_{1/2} + \frac{1}{3} M^1_{1/2} - \frac{1}{3} M^1_{3/2}|^2 dR \tag{1b}$$

$$\sigma_3 \equiv \sigma(n_1p_2 \to p_3(p_4\rho^-)) = \frac{2}{27} \int |2\, M^1_{1/2} + M^1_{3/2}|^2 dR \tag{1c}$$

$$\sigma_4 \equiv \sigma(p_1n_2 \to p_3(n_4\rho^o)) = \frac{1}{3} \int |M^0_{1/2} + \frac{1}{3} M^1_{1/2} + \frac{2}{3} M^1_{3/2}|^2 dR \tag{1d}$$

$$\sigma_5 \equiv \sigma(n_1p_2 \to p_3(n_4\rho^o)) = \frac{4}{27} \int |M^1_{1/2} - M^1_{3/2}|^2 dR \tag{1e}$$

$$\sigma_6 \equiv \sigma(p_1p_2 \to n_3(p_4\rho^+)) = \frac{2}{3} \int |M^1_{3/2}|^2 dR \tag{1f}$$

$$\sigma_7 \equiv \sigma(p_1p_2 \to p_3(n_4\rho^+)) = \frac{2}{3} \int |M^0_{1/2} - \frac{1}{3} M^1_{1/2} + \frac{1}{3} M^1_{3/2}|^2 dR \tag{1g}$$

The internal parentheses indicate to which final state nucleon the ρ is associated. Kinematical factors are included in the amplitudes and the integration over dR stands for summation of helicities and integration over a region of phase space. The relations are of course identical to those for single pion production, but since the ρ is observed by its decay products, different charge channels are observable for π and ρ production.

We will in the subsequent analysis use only total cross sections, i.e. cross sections integrated over the full phase space and summed over helicities. The corresponding isospin cross sections and the interference terms are denoted as follows:

$$\begin{aligned} m_0 &\equiv \int < |M^0_{1/2}|^2 > dR, & m_1 &\equiv \int < |M^1_{1/2}|^2 > dR \\ m_3 &\equiv \int < |M^1_{3/2}|^2 > dR, & m_{01} &\equiv \int < \mathrm{Re}(M^{0*}_{1/2}\, M^1_{1/2}) > dR \\ m_{03} &\equiv \int < \mathrm{Re}(M^{0*}_{1/2}\, M^1_{3/2}) > dR, & m_{13} &\equiv \int < \mathrm{Re}(M^{1*}_{1/2}\, M^1_{3/2}) > dR \end{aligned} \tag{2}$$

These quantities are constrained by the following inequalities [2, 3]:

$$m_0 \geq 0, \quad m_1 \geq 0, \quad m_3 \geq 0 \tag{3a}$$

$$\begin{vmatrix} m_{01} & m_{01} \\ m_{01} & m_1 \end{vmatrix} \geq 0, \quad \begin{vmatrix} m_3 & m_{03} \\ m_{03} & m_0 \end{vmatrix} \geq 0, \quad \begin{vmatrix} m_1 & m_{13} \\ m_{13} & m_3 \end{vmatrix} \geq 0, \tag{3b}$$

$$\begin{vmatrix} m_0 & m_{01} & m_{03} \\ m_{01} & m_1 & m_{13} \\ m_{03} & m_{13} & m_3 \end{vmatrix} \geq 0. \tag{3c}$$

There is one measured cross section less than the number of integrated isospin amplitudes and interference terms. In accordance with ref. [1] we therefore choose the interference term m_{13} as a "free" parameter (i.e. constrained only by the inequalities 3a-3c), and the other quantities (2) are then given as linear functions of m_{13} as follows:

$$m_0 = -2x + \frac{3}{4}(2\sigma_1 + 2\sigma_3 + 2\sigma_4 - 5\sigma_5) \tag{4a}$$

$$m_1 = -2x + \frac{9}{4}(2\sigma_3 - \sigma_5) \tag{4b}$$

$$m_3 = 4x + \frac{9}{2}(-\sigma_3 + 2\sigma_5) \tag{4c}$$

$$m_{01} = 2x + \frac{3}{4}(-3\sigma_1 + 2\sigma_2 - 2\sigma_3 - \sigma_4 + 4\sigma_5) \tag{4d}$$

$$m_{03} = -x + \frac{3}{4}(-\sigma_2 + \sigma_3 + 2\sigma_4 - 2\sigma_5) \tag{4e}$$

$$m_{13} = x \tag{4f}$$

The range of variation of the isospin cross sections (4a)-(4f) is then determined by the region to which $m_{13} = x$ is constrained by the inequalities (3a)-(3c).

As mentioned above we would also like to analyse the reactions in terms of the double peripheral scheme given in fig. 1b, where the corresponding amplitudes M^{01}, M^{10} and M^{11} are defined.

It should be pointed out that the exchange I_x of the single peripheral representation corresponds to I_1 of the double peripheral representation.

The relation between the two sets of amplitudes is given by:

$$M^{01} = M^{0}_{1/2} \tag{5a}$$

$$M^{10} = -\frac{1}{3}M^{1}_{1/2} - \frac{2}{3}M^{1}_{3/2} \tag{5b}$$

$$M^{11} = \sqrt{\frac{2}{3}}M^{1}_{1/2} - \sqrt{\frac{2}{3}}M^{1}_{3/2} \tag{5c}$$

The relations (5) are given in ref. [4], but with a different normalization of the double peripheral amplitudes, denoted P, Q and R respectively. The relation between the two sets of amplitudes is $M^{01} = \sqrt{\frac{3}{2}}\,P$, $M^{10} = -\sqrt{\frac{3}{2}}\,Q$ and $M^{11} = 3R$.

In terms of the cross sections $\sigma_1 - \sigma_5$ and the parameter $y = m^{10,11}$, one gets the following expressions for the integrated quantities:

$$m^{01} \equiv \int <|M^{01}|^2> dR = -\sqrt{\frac{2}{3}}\,y + \frac{3}{4}(2\sigma_1 - 2\sigma_3 + 2\sigma_4 + \sigma_5) \tag{6a}$$

$$m^{10} \equiv \int <|M^{10}|^2> dR = \sqrt{\frac{2}{3}}\,y + \frac{3}{4}(2\sigma_3 - \sigma_5) \tag{6b}$$

$$m^{11} \equiv \int <|M^{11}|^2> dR = \frac{9}{2}\sigma_5 \tag{6c}$$

$$m^{01,10} \equiv \int < Re(M^{01*}M^{10}) > dR = \frac{3}{4}(\sigma_1 - \sigma_4) \tag{6d}$$

$$m^{01,11} \equiv \int < Re\,(M^{01*}M^{11}) > dR = y + \frac{3}{2}\sqrt{\frac{3}{2}}(-\sigma_1 + \sigma_2 + \sigma_3 - \sigma_4 - \sigma_5) \tag{6e}$$

$$m^{10,11} \equiv \int < Re\,(M^{10*}M^{11}) > dR = y \tag{6f}$$

The cross sections (6a)-(6f) of course fulfil inequalities similar to those for the single peripheral representation.

We note that in this representation one isospin cross section and one interference term are directly measured by the observed cross sections.

To find the importance of the different isospin amplitudes, one must consider their contributions to the observed cross sections σ_i. These contributions are independent of the normalization chosen, while that is of course not true for the isospin cross sections. In particular it is interesting to find the contributions from the various amplitudes to the total cross section $\sum_{i=1}^{7} \sigma_i$, since this would be a measure of the relative importance of the corresponding exchange mechanisms for the processes considered. These contributions, $F(M_I^{I_x})$ and $F(M^{I_1 I_2})$ for the single and double peripheral diagrams respectively, are given by the following expressions:

$$F(M_I^{I_x}) = \frac{2I+1}{2I_x+1} \int |M_I^{I_x}|^2 \, dR \tag{7.1}$$

$$F(M^{I_1 I_2}) = \frac{6}{(2I_1+1)(2I_2+1)} \int |M^{I_1 I_2}|^2 dR \tag{7.2}$$

The normalization chosen is such that $\sum_{i=1}^{7} \sigma_i = \sum_{II_x} F(M_I^{I_x}) = \sum_{I_1 I_2} F(M^{I_1 I_2})$.

With obvious short-hand notations for the contributions F we thus have:

$$\sum_{i=1}^{7} \sigma_i = 2m_0 + \frac{2}{3} m_1 + \frac{1}{3} m_3 = F_0 + F_1 + F_3$$

$$= 2m^{01} + 2m^{10} + \frac{2}{3} m^{11} = F^{01} + F^{10} + F^{11} .$$

2.2 $N_1 N_2 \to N_3 N_4 f^0$

Referring to the peripheral isospin diagram of fig. 2a, we define the amplitudes $M_I^{I_x}$ for single f^0 production in the same way as in the case of ρ production. Since f^0 is isoscalar, the isospin of the nucleon-f^0 system must be $I = \frac{1}{2}$ and two independent isospin amplitudes $M_{1/2}^0$ and $M_{1/2}^1$ are necessary and sufficient.

If charge symmetric reactions are neglected, there are three different charge channels in NN reactions leading to NNf^0 final states. The relations between the cross sections and the isospin amplitudes are:

$$\sigma_1 \equiv \sigma(p_1 p_2 \rightarrow p_3(p_4 f^0)) = \int |M^0_{1/2} - \frac{1}{3} M^1_{1/2}|^2 dR \tag{8a}$$

$$\sigma_2 \equiv \sigma(p_1 n_2 \rightarrow p_3(n_4 f^0)) = \int |M^0_{1/2} + \frac{1}{3} M^1_{1/2}|^2 dR \tag{8b}$$

$$\sigma_3 \equiv \sigma(p_1 n_2 \rightarrow n_3(p_4 f^0)) = \frac{4}{9} \int |M^1_{1/2}|^2 dR \tag{8c}$$

The notation and conventions are the same as for ρ-production in section 2.1.

The set of equations can be solved to give the following expressions:

$$m_0 = \frac{1}{2}\sigma_1 + \frac{1}{2}\sigma_2 - \frac{1}{4}\sigma_3 \tag{9a}$$

$$m_1 = \frac{9}{4}\sigma_3 \tag{9b}$$

$$m_{01} = -\frac{3}{4}\sigma_1 + \frac{3}{4}\sigma_2 \tag{9c}$$

Finally we turn to the double exchange diagrams shown in fig. 2b, and denote the isospin amplitudes by $M^{I_1 I_2}$ where I_1 and I_2 refer to the isospins of the two exchanges.

We choose the normalization such that the relation between the two sets of amplitudes is

$$M^0_{1/2} = M^{00} \tag{10a}$$

$$M^1_{1/2} = \sqrt{\frac{1}{3}}\, M^{11} \tag{10b}$$

Since f^0 is an isoscalar particle the contributions $F(M^{I_x}_{1/2})$ and $F(M^{I_1 I_2})$ to the total cross section $\sum_{i=1}^{3} \sigma_i$ are equal for the two sets of amplitudes and they are given by

$$F(M^{I_x}_{1/2}) = \frac{2}{2I_x + 1} \int |M^{I_x}_{1/2}|^2 dR \tag{11a}$$

$$F(M^{I_1 I_2}) = \frac{2}{(2I_1 + 1)(2I_2 + 1)} \int |M^{I_1 I_2}|^2 dR \tag{11b}$$

Again the normalizations are such that $\sum_{i=1}^{3} \sigma_i = \sum_{I_x} F(M^{I_x}_{1/2}) = \sum_{I_1 I_2} F(M^{I_1 I_2})$.

3. EXPERIMENTAL INFORMATION

The present analysis is based upon data from the Scandinavian 19 GeV/c pp and pd bubble chamber experiments. From the pp experiment data on the channel $pp \to pp\pi^+\pi^-$ are needed, and these data are obtained from 3078 events for this reaction. Further details about this reaction and the pp experiment are found in ref. [5-7]. A cross section for the reaction $pp \to pp\rho^o$ and a revised [5] cross section for $pp \to ppf^o$ are evaluated in section 3.2 below.

3.1 The pd experiment

The pd data to be used are preliminary and are based on ca. 40 000 measured events, which is the part of our deuterium film (ca. 75 %) analysed until now. The scanning, measuring and reconstruction procedures have been described in ref. [1], and we give only those details that are of particular importance for the determination of the ρ- and f^o-production cross sections.

The events have been fitted to the following final states:

$pd \to p\,p\,\pi^-$	p_{spec}	(a)
$pd \to p\,p\,\pi^-\,\pi^o$	p_{spec}	(b)
$pd \to p\,n\,\pi^+\,\pi^-$	p_{spec}	(c1)
$\to p\,p\,\pi^+\,\pi^-$	n_{spec}	(c2)
$pd \to p\,d\,\pi^+\,\pi^-$		(d)
$pd \to p\,d\,\pi^+\,\pi^-\pi^o$		(e)
$pd \to n\,d\,\pi^+\pi^+\pi^-$		(f)

The spectator is defined as the nucleon with the smallest laboratory momentum, and channels (c1) and (c2) are thus identical except for the labeling of different nucleons as the spectator.

Of the kinematically acceptable hypotheses only those consistent with the observed track bubble densities were retained. To purify the sample further, additional criteria were applied as described in ref. [1], but still ca. 30 % of the events had ambiguous interpretations. The ambiguities have for the purpose of extracting a reliable sample of the reactions $pn \rightarrow pp\pi^{-}\pi^{0}$ and $pn \rightarrow pn\pi^{+}\pi^{-}$ been treated in the following way:

1) Hypotheses competing with (a), which is a 4C hypothesis, are rejected.
2) An event with an ambiguity between a coherent and a non-coherent hypothesis is classified as coherent if it is a 4-prong event, otherwise both interpretations are accepted with proper weights.
3) Ambiguities between the π^{0}-channel (b) and the neutron channel (c), and also the internal ambiguities of channel (c), have been resolved by favouring the hypothesis with the most peripherally produced nucleons.

There is also the possibility of wrong assignments between the proton and neutron-spectator channels (c1) and (c2) where we choose as the spectator the nucleon with the smallest momentum. From the channel $pp \rightarrow pp\pi^{+}\pi^{-}$ observed with hydrogen target [5-7], we can estimate the cross section for the neutron spectator channel, and we find them to be equal within errors. This does not mean that we always make the right choice but only that there is no net flux from either channel.

The above procedure resulted in 810 accepted events for the π^{0}-channel (b) and 3064 events for the neutron channel (c1), when a probability cut of 10 % has been applied.

3.2 Cross sections

To extract free pn cross sections from the corresponding pd cross sections we rely on the spectator model procedure as described in our earlier report [1]. A 5 % correction for Glauber screening has been applied. No correction for the Pauli exclusion principle has been made since it is assumed to be negligible.

In fig. 3 we show the effective mass distributions of the two pions for the following four channels of interest:

$$pp \rightarrow pp\,\pi^+\pi^- \qquad (A)$$

$$pn \rightarrow pp\,\pi^-\pi^0 \qquad (B)$$

$$pn \rightarrow p_F n_B\,\pi^+\pi^- \qquad (C)$$

$$pn \rightarrow p_B n_F\,\pi^+\pi^- \qquad (D)$$

F and B label the directions forward and backward in the CM system relative to the beam direction.

A ρ signal is clearly seen in the reactions (B), (C) and (D), while it in reaction (A) appears as a shoulder. To show that ρ and f^0 production exist and to calculate the cross sections, different cuts to the data have been applied in the ρ and f^0 cases as described below.

3.2.1 ρ cross section

In fig. 4 the same two-pion mass distributions as in fig. 3 are displayed with the additional requirement that the M_0 $(N + 2\pi)$ mass is above 1750 MeV [illegible], where M_0 $(N + 2\pi)$ represents the mass of the $(N + 2\pi)$-combination with the minimum momentum transfer. The ρ-signal is now clearly seen also in the reaction $pp \rightarrow pp\,\pi^+\pi^-$.

To obtain the cross sections for ρ-production in reactions (A)-(D), we have fitted to the mass distributions of fig. 4 an incoherent sum of a relativistic Breit Wigner term * and a peripheral background term. (For the $\pi^+\pi^-$ mass distributions a Breit Wigner term for f^0 is included.) The background terms are obtained by Monte Carlo generated events as a peripheral phase space including transverse momentum cut-off, leading particle effect and pronounced resonance production. This peripheral phase space describes all relevant distributions well, in particular the low mass peak of reaction (D) as seen from the curve of fig. 3d. The values of the central masses and the widths of ρ and f^0 were fixed to those of tables 1 and 2. The results of the fits are given in table 1. The best fits are shown as full curves

---

* The Breit Wigner amplitude squared is parametrized as

$$BW \propto \frac{M\, m_0\, \Gamma\, \Gamma_0}{(M^2 - m_0^2)^2 + m_0^2\,\Gamma^2} \quad \text{with } \Gamma = \Gamma_0\, \frac{m_0}{M} \left(\frac{q}{q_0}\right)^{2\ell+1} \text{[illegible]}.$$

drawn to the mass plots of fig. 4, and the broken curves indicate the fitted background terms. No correction has been applied to the ρ cross sections to account for the effect of the mass cut.

It should be pointed out that in the channels where similar fits easily can be made to the uncut mass distributions of fig. 3, compatible results are obtained.

As described in section 2 the produced ρ must be associated with one of the final state nucleons to obtain the cross sections needed for the isospin analysis. To show to what extent ρ actually clusters to one of the nucleons, we display in fig. 5 the Dalitz plot of $M^2(p_F\pi^-\pi^0)$ versus $M^2(p_B\pi^-\pi^0)$ in channel (B) where the $(\pi^-\pi^0)$-mass is restricted to the ρ interval (660-860) MeV.

Although the background events to some extent hide the structure of the events with genuine ρ production, there is a clear tendency for the produced ρ to be associated with one of the nucleons. Similar features are seen in the other three channels.

From the definitions of $\sigma_1 - \sigma_5$ in section 2, we see that σ_1 is simply half the cross section for ρ production in reaction (A). From charge symmetry it is clear that the reactions with ρ^0 production in channels (C) and (D) are the sums of two charge symmetric reactions where ρ^0 is associated with one of the nucleons. Therefore the cross sections σ_4 and σ_5 may also be obtained as half the cross sections for ρ production in channel (C) and (D), respectively. However, to evaluate cross sections σ_2 and σ_3 one has to define some way to associate the ρ^- with either the target proton or the beam proton. In the case of pion production this has been done in a variety of ways. In ref. [1] a new procedure was adopted in which the distribution of $\cos\theta$ of the produced pion in the CM system was used to associate the meson with one of the nucleons.

We have therefore plotted in fig. 6 the distribution of $\cos\theta_{CM}$ of the $(\pi^-\pi^0)$-system from reaction $pn \to pp\pi^-\pi^0$ where the $(\pi^-\pi^0)$-mass is confined to the ρ-band. The distribution of the background events is assumed to be described by the Monte Carlo generated events discussed above. These generated events describe the $\cos\theta_{CM}$ distribution of the events below and above the ρ-band very well. The arrow in fig. 6b, where the subtracted distribution is plotted, indicates the separation point. The ratio between the number of events produced on the beam and target vertices obtained in this way, is then used to derive the cross sections σ_2 and σ_3 from the value of $\sigma_2 + \sigma_3 = \sigma(pn \to pp\rho)$ given in table 1.

The cross sections $\sigma_1 - \sigma_5$ computed as described above, are given in table 3 together with corresponding cross sections at other energies. The errors are those from the fits. The cross sections at other energies are discussed in section 5.

3.2.2 f^0 cross sections

The cross sections for single f^0 production are obtained from reactions (A) - (C) and (D) above, and the corresponding $\pi^+\pi^-$ mass distributions are shown in fig. 7 with a similar threshold cut as was applied for ρ-production, i.e. only events with $M_0(N + 2\pi) > 2250$ MeV are accepted.

Although the signals for f^0 production are rather weak in these plots, we have made similar fits to the mass distributions as in the ρ case. In the fits we used the values of the central masses and widths of f^0 and ρ^0 that are given in tables 2 and 1 respectively. The results of the fits are given in table 2 and as full curves in fig. 7. The broken curves represent the fitted background terms used for the different reactions.

The cross sections needed for the isospin analysis $\sigma_1 - \sigma_3$ are simply obtained as half the cross sections found in the fits, and are given in table 4 together with available data at other energies. The errors of the cross sections are those from the fits. All the cross sections in table 4 are corrected for unobserved decay modes of f^0 (branching ratio of $f^0 \to \pi^+\pi^-$ to all is (55 ± 5) % [10]).

4. EXPERIMENTAL RESULTS AT 19 GeV/c

4.1 $N_1 N_2 \to N_3 (N_1 \rho)$

The five cross sections $\sigma_1 - \sigma_5$ of table 3 at 19 GeV/c were used in equations (4a)-(4f) to find the intervals to which the isospin cross sections $m_0 - m_{13}$ are constrained by the inequalities (3a)-(3c). The results are given in table 5 and the errors attached to the intervals stem from the errors of the observed cross sections. We mentioned in section 2 that it would be interesting to discuss this reaction also in the double peripheral representation. The relations (6a)-(6f) were used to calculate the corresponding intervals of the isospin cross sections of the double exchange diagrams. The results are given in table 5 together with those for the single exchange diagrams. The same results are also displayed in fig. 8 where we have plotted the different isospin cross sections as functions of m_{13} and $m^{10,11}$.

Following ref. [1] we introduce the normalized interference terms β_{ij} defined by

$$m_{ij} = \beta_{ij} \sqrt{m_i m_j}$$

for single exchange diagrams, and in a corresponding way for the double exchange diagrams. We note that $|\beta_{ij}| \leq 1$, and that the values of these normalized interference terms are determined by the coherence of the amplitudes and by their relative phase. The intervals of the β's are given in table 5.

We will now compare these results with those obtained earlier for single pion production in terms of the isospin cross sections and the normalized interference terms.

For the single exchange representation we recall that the main results were a clear dominance of the isoscalar exchange cross section m_0, and that the normalized interference terms β_{03} and β_{13} were close to zero while β_{01} was large in magnitude and negative. It is clear from fig. 8 and table 5 that m_0 is not dominating in ρ production contrary to the pion case. The normalized interference terms are seen to be essentially undetermined. Transformed to the double exchange representation the cross section $m^{01} = m_0$ again dominated in the pion case but not in the ρ case.

To present the relative importance of the different amplitudes we plot in fig. 9 the contributions $F(M_I^{I_x})$ and $F(M^{I_1 I_2})$ to the total cross section $\sum_{i=1}^{7} \sigma_i$. For the double exchange diagram we also plot the sum $F^{01} + F^{10} = 3\sigma_1 + 3\sigma_4$. Since $F^{11} = 3\sigma_5$, both F^{11} and the sum $F^{01} + F^{10}$ are constants, independent of the variable $y = m^{10,11}$. From fig. 9b, where also the errors are indicated, we observe that F^{11} has a significantly lower cross section than $F^{01} + F^{10}$. Thus describing the reactions $N_1 N_2 \rightarrow N_3 (N_4 \rho)$ in a double peripheral diagram, the amplitudes with double isovector exchange are less important at 19 GeV/c than the amplitudes which include isoscalar exchange. This tendency was, however, much stronger in the case of single pion production.

4.2 $N_1 N_2 \rightarrow N_3 N_4 f^0$

The cross sections σ_1, σ_2 and σ_3 of table 4 at 19 GeV/c were used in the equations (8a)-(8c) to find the isospin cross sections m_0 and m_1 and the interference term m_{01}. The values are given in table 6, where we also give the value of the normalized interference term ϑ_{01}. The values of the contributions $F(M_{1,2}^{I_x})$ to the total cross section $\sum_{i=1}^{3} \sigma_i$ are given in table 6, with obvious shorthand notation.

As can be seen from table 6, the two isospin cross section contributions F_0 and F_1 are about equal, with F_0 slightly larger than F_1. We also note that the normalized interference term ϑ_{01} is small. The relatively large errors on these quantities do not, however, allow any firm conclusions to be drawn.

5. ENERGY DEPENDENCE OF THE AMPLITUDES

5.1 $N_1N_2 - N_3N_4\rho$

The cross sections for single ρ production in pN-collisions in the momentum range 4-25 GeV/c are given in table 3 and fig. 10. As can be seen most of the cross sections are for the reaction $pp \to pp\rho^o$, and only very few cross sections for ρ-production in pn collisions are available. In the footnote of table 3 it is indicated that some of the pp cross sections are published ones, while the others have been extracted as described in the footnote of table 3 by using the World Collaboration Data Summary Tape on the reaction $pp \to pp\pi^+\pi^-$ [11]. In some of the pp experiments, for which we now give the cross section σ_1, ρ-production has not been claimed by the authors (see footnote of table 3). However, the use of the mass cut introduced by Blobel et al. [8], simplifies the extraction of these cross sections. The only pn cross sections available are the full set of cross sections $\sigma_2-\sigma_5$ at 19 GeV/c (this exp.) and σ_5 and $\sigma_2+\sigma_3$ at 7 GeV/c [18].

Analyses similar to that at 19 GeV/c, which would be valuable to perform also at other energies, are therefore not possible.

We will, however, follow the procedure of ref. [1] and assume a parametrization of the isospin cross sections and the interference terms as functions of energy, since all available data may then be used in a total fit to determine the integrated amplitude terms and their energy dependence.

Starting with the single exchange representation it seems natural to try the same parametrization as we used for single pion production [1],

$$
\begin{aligned}
m_i &= k_i\, p_{lab}^{n_i} \\
\beta_{ij} &= \frac{m_{ij}}{\sqrt{m_i m_j}} = \text{constant}
\end{aligned}
\qquad (12)
$$

which contains nine parameters to be determined.

Due to phase space effects this parametrization will generally predict larger cross sections than the observed ones at low energies. For single pion production we therefore restricted ourselves to primary momenta above 6 GeV/c. For ρ production the phase space effects are appreciable even for higher energies than 6 GeV/c, and we therefore choose to "correct" for the phase space effects by writing [25]:

$$\sigma_i = \sigma_i' \cdot \frac{(\text{phase space volume})}{\text{constant} \cdot p_{lab}} \qquad (13)$$

where σ_i are the observed cross sections and the constant is chosen such that the phase space factor

$$\frac{\text{phase space volume}}{\text{constant} \cdot p_{lab}}$$

tends to 1 as $p_{lab} \to \infty$. The primed quantities σ_i' we refer to as phase space modified cross sections.

To see the effect of this modification we show in a log-log plot in fig. 11 the cross sections σ_1 of the table 5 as function of p_{lab} and the corresponding modified cross sections σ_1'. It is obvious that the results of the subsequent analysis to some extent will depend on the choice of the phase space factor.

We have tried to fit the parameters in (5.1) to the modified cross sections σ_i' but no fit was obtained. The reason for this may be that the parametrization is not correct. Another difficulty is that there are so few pn cross sections.

Turning to the double peripheral representation we start by mentioning that the parametrization (12) gives a good fit to the single pion production data of ref. [1]. We therefore try this parametrization also for the ρ production data. The result of this fit is given in table 7 and fig. 12.

To summarize the main features we note that

A. The fit is acceptable from a statistical point of view, but the values of the fitted parameters as well as their errors depend critically on the few pn cross sections given.

B. The isospin cross section m^{01} has a weak energy dependence. The term m^{01}, which is equal to the isoscalar exchange cross section m_0 of the single exchange scheme, is likely to be pomeron (P) dominated at high energies. From the weak energy dependence a pair of exchange trajectories including $(P+\rho)$ is expected to contribute largely to m^{01} also in our energy range.

C. The isospin cross sections m^{10} and m^{11} have about equal energy dependence (the slope parameters $n \approx -1$) and $F(M^{10})$ is the dominating contribution. The observation that the isospin cross section with double isovector exchange is of minor importance, agrees with the results at 19 GeV/c in section 4.1.

As we pointed out in section 2 the exchange labeled I_1 corresponds to the exchange I_x of the single peripheral representation. Taking the peripheral nature of the reactions into account it then follows that the trajectories corresponding to I_1 must have a higher intercept than the ones corresponding to I_2. This must obviously be true for m^{10} since it is the leading term but must hold for m^{11} as well since one cross section σ_5 depends exclusively on m^{11}. Possible pairs of exchanges like $(\pi+\omega)$ and $(A_2+\omega)$ for m^{10} and $(\rho+\rho)$ and $(\pi+A_2)$ for m^{11} are thereby not allowed. Equal intercepts for m^{11} is also excluded from the fact that there is a dip in the CM rapidity distribution for ρ^o at $y = 0$. With the observed energy dependence we are therefore left with $\rho+\eta$ and $A_2+\pi$ as the most probable dominating exchanges for m^{10} and m^{11} respectively.

D. The two normalized interference terms involving double isovector exchange, $\beta_{01,11}$ and $\beta_{10,11}$, are large in magnitude and with opposite signs.

It is now interesting to compare these results with two earlier analyses of single ρ production [8, 18].

Blobel et al. [8] have used pp data at 12 and 24 GeV/c and performed a double-Regge analysis of the channel $pp \to pp\rho^o$. From the energy dependence of their cross sections they can exclude a dominating pomeron contribution in accordance with our observations. In the CM rapidity of ρ^o they further observe a dip at $y = 0$. They conclude that vector meson-like (ω) and pion-like (π) trajectories should be the dominating pair of exchanges; (ω and π stand for trajectories with intercept $\alpha(o) \approx 0.5$ and $\alpha(o) \approx 0$ respectively).

From equations (6) one can see that m^{01} and m^{10} have equal contributions to the cross section $\sigma(pp \to pp\rho^o)$. Our results are therefore in fair agreement with that of Blobel et al., provided their vector meson-like and pion-like trajectories are taken as ρ and η respectively.

At 7 GeV/c Yekutieli et al. [18] discuss the mechanism for single ρ production in pn collisions and conclude that a diagram with double isovector exchange explains the process. This does not agree with our results since the contribution to the total pn cross section $\sum_{i=2}^{5}\sigma_i$ * from m^{11} is less than 50 at 7 GeV/c (interference terms neglected).

When we compare the present results for ρ production with those for pion production [1], we see a clear difference in the contribution from single isoscalar exchange to the two processes. For single pion production the isoscalar exchange was found to be the leading mechanism above 7 GeV/c, and since $F(M_0) < F(M^{01})$ we find that this is not the case for ρ production.

5.2 $N_1N_2 \rightarrow N_3N_4f^0$

The available cross sections for single f^0 production in pN collisions are given in table 7 and for completeness also plotted in fig. 10 as function of the beam momentum. The footnote of table 7 tells which of the pp cross sections are found in the literature and which have been extracted by us from the World DST [11]. Primarily because of lack of statistics the errors of the cross sections are relatively large for most of the experiments, but still some discrepancies seem to exist between the cross sections. It is interesting to note that cross sections for f^0 production in pn collisions are here given for the first time.

It would now have been natural to try a parametrization of the isospin cross sections similar to that for ρ production, in order to obtain the energy dependence of the cross sections for the two possible exchanges, i.e. the double isovector and double isoscalar exchanges. Particularly interesting would it be to see if there is any indication of double Pomeron exchange [8]. The fact that pn cross sections exist only at one energy eliminates the possibilities of a fit with the parametrization indicated.

---

* $\sum_{i=2}^{5}\sigma_i = (\frac{5}{3}m^{01} + m^{10} - \frac{2}{3}m^{01,10}) + \frac{1}{3}m^{11} - \frac{2}{3}\sqrt{\frac{2}{3}}\,m^{10,11}$

6. SUMMARY

The aim of this paper is to use the method of cross channel isospin analysis to discuss the mechanism of single ρ and f^0 production in nucleon-nucleon collisions.

We present data on single ρ and f^0 production in pn collisions at 19 GeV/c. Cross sections for the reaction $pn \to pnf^0$ have not earlier been published. Some cross sections for the reaction $pp \to pp\rho^0$ have been extracted from the World Collaboration DST [11] on the reaction $pp \to pp\pi^+\pi^-$.

The analysis at 19 GeV/c, performed both in a single and in a double exchange representation, does not allow us to decide if any isospin amplitude dominates the process of single ρ and f^0 production at this energy. It shows, however, that when the process is considered in the double peripheral representation, double isovector exchange plays a minor role for ρ production and that both double isovector and double isoscalar exchange mechanisms seem to contribute to single f^0 production.

To determine the energy variation of the isospin cross sections and the interference terms, using all available data, we have parametrized the isospin cross sections as power laws $\sim p_{lab}^{n_i}$ and the normalized interference terms as constants (eq. 12). In the case of f^0 production too few pn cross sections exist to determine the parameters. In the ρ-case an acceptable fit is obtained in the double peripheral representation, but the results depend critically on the few available pn cross sections.

For ρ production at energies below 25 GeV/c the result of the fit leads to the following features concerning the production amplitudes:

i The $(I_1 = 0, I_2 = 1)$-amplitude, corresponding to single isoscalar exchange in the single peripheral representation, is not dominating and has a weak energy dependence in accordance with isoscalar exchange being Pomeron dominated.

ii The two other amplitudes $(I_1 = 1, I_2 = 0)$ and $(I_1 = I_2 = 1)$, which are related to isovector exchange in the single exchange scheme, have about the same energy dependence (slope parameter $n \cong -1$).

iii The $(I_1 = 1, I_2 = 0)$-exchange is the leading mechanism compared with $(I_1 = I_2 = 1)$-exchange, and could be dominated by $(\rho + \eta)$-exchange.

Interpreting the results in the single peripheral representation, we find that the isoscalar exchange mechanism plays a less importante role for single ρ than for single π production in the energy range considered.

More data, especially for the pn reactions are needed in order to reach more definite conclusions concerning the exchange mechanism of single ρ production in nucleon-nucleon collisions using this type of analysis. For single f^0-production new cross sections from pn-reactions at other energies than 19 GeV/c are necessary to obtain the energy variation of the isospin cross sections and possibly isolate the leading exchanges.

ACKNOWLEDGEMENT

We wish to thank the staffs of the CERN Proton Synchrotron, of the 2m hydrogen bubble chamber and of the U5 beam for their efforts during the exposures for this experiment.

Our thanks are also due to the scanning and measuring staffs at our four universities and the staffs of the computing centers in Copenhagen, Helsinki, Oslo and Stockholm.

Supports from Research Councils in Denmark, Finland, Norway and Sweden are gratefully acknowledged.

LIST OF REFERENCES

1 E. Dahl-Jensen et al., Nucl.Phys. B87 (1975) 426.

2 Z. Koba, R. Møllerud and L. Veje, Nucl.Phys. B26 (1971) 134.

3 J. Bjørneboe, Z. Koba and N. Törnqvist, Phys.Letters 34B (1971) 638.

4 Z. Koba, Acta Physica Polonica B3 (1971) 789.

5 Scandinavian Bubble Chamber Collaboration, Report to the Internat. Conference on High Energy Physics, Vienna, 1968.

6 H. Bøggild et al., Nucl.Phys. B27 (1971) 285.

7 H. Johnstad et al., Nucl.Phys. P12 (1972) 558.

8 V. Blobel et al., Nucl.Phys. B69 (1974) 237.

9 J.D. Jackson, Nuovo Cimento 34 (1964) 1644.

10 Particle Data Group, Review of particle properties (1974).

11 The World Collaboration on the reaction $pp \rightarrow pp\pi^{+}\pi^{-}$, Common Data Summary Tape (1970).

12 S. Coletti et al., Nuovo Cimento 11A (1967) 480.

13 A.P. Colleraine et al., Phys.Rev. 161 (1967) 1387.

14 G. Alexander et al., Phys.Rev. 154 (1967) 1284.

15 W. Chinowsky et al., Phys.Rev. 171 (1968) 1421.

16 E. Colton and P. Schlein, Phys.Rev. 3 (1971) 1063.

17 G. Yekutieli et al., Nucl.Phys. B18 (1970) 301.

18 G. Yekutieli et al., Phys.Letters 34B (1971) 101.

19 D. Grether et al., Bull.Am.Phys.Soc. 12 (1967) 10.

20 S.P. Almeida et al., Phys.Rev. 174 (1968) 1638.

21 J. Le Guyader et al., Nucl.Phys. B35 (1971).

22 J.G. Rushbrooke, J.R. Williams, Phys.Rev.Letters 22 (1969) 248.

23 R.A. Jesperson et al., Phys.Rev.Letters 21 (1968) 1368.

24 R. Ehrlich et al., Phys.Rev.Letters 21 (1968) 1839.

25 J.D. Hansen, W. Kittel and D.R.O. Morrison, Nucl.Phys. B25 (1971) 605.

FIGURE CAPTIONS

Fig. 1 Definition of the cross channel isospin amplitudes for the reaction $N_1N_2 \to N_3(N_4\rho)$ for
a) single exchange diagrams
b) double exchange diagrams

Fig. 2 The same as fig. 1 for the reaction $N_1N_2 \to N_3(N_4f^0)$.

Fig. 3 Mass distributions $M(\pi\pi)$ for reactions (A)-(D). For reactions (B), (C) and (D) a probability cut of 10 % has been applied. The curve for the reaction $pn \to p_B n_F \pi^+\pi^-$ represents the Monte Carlo generated events (see text), including a Breit Wigner representation of ρ^0, (two pages).

Fig. 4 $M(\pi\pi)$ distributions of events for which $M_0(N\pi\pi) > 1750$ MeV, where $M_0(N\pi\pi)$ is the mass of the $(N\pi\pi)$-combination with minimum momentum transfer. The full curves represent the best fits of a background + Breit Wigner terms of ρ and f^0. The broken curves show the fitted background terms, (two pages).

Fig. 5 Dalitz plot of $M^2(p_F\pi^-\pi^0)$ versus $M^2(p_B\pi^-\pi^0)$ for the channel $pn \to p_F p_B \pi^-\pi^0$ where p_F and p_B label the protons going forward and backward in the CM system, respectively. $M(\pi^-\pi^0)$ is confined to the ρ region (660-880) MeV.

Fig. 6 a) Distribution of $\cos\theta_{CM}$ of the $(\pi^-\pi^0)$-system in the reaction $pn \to pp\pi^-\pi^0$, when $M(\pi^-\pi^0)$ is confined to the ρ-region (660-880) MeV. The hatched distribution represents the Monte Carlo generated background (see text) normalized according to estimated ρ^- cross sections.

b) The difference between the two distributions in a). The arrow indicates the separation point.

Fig. 7 $M(\pi^+\pi^-)$ distributions of events for which $M_0(N\pi\pi) > 2250$ MeV, where $M_0(N\pi\pi)$ is the mass of the $(N\pi\pi)$-combination with minimum momentum transfer. The full curves represent the best fits of a background + Breit Wigner terms of ρ^0 and f^0. The broken curves show the fitted background terms.

Fig. 8 The isospin cross sections and the interference terms as functions of the free parameter x in the interval to which x is confined, for

a) single exchange isospin diagrams

b) double exchange isospin diagrams

Fig. 9 The contributions $F(M_I^{I_x})$ and $F(M^{I_1 I_2})$ to the total cross section $\sum_{i=1}^{7} \sigma_i$

Fig. 10 Cross sections as functions of the beam momentum for

a) $\sigma_1 = (pp \rightarrow p(p\rho^0))$ from table 3

b) $\sigma_1 = (pp \rightarrow p(pf^0))$ from table 4

Fig. 11 The cross section $\sigma_1 = (pp \rightarrow p(p\rho^0))$ from table 3 and the corresponding phase space modified cross section σ_1' as function of the beam momentum. The curves represent the fit to the modified cross sections σ_1' in the double peripheral scheme (see text).

Fig. 12 Results from the fit to all phase space modified cross sections σ_i' for single ρ production. The contributions F^{01}, F^{10} and F^{11} to the total cross section $\sum_{i=1}^{7} \sigma_i'$

TABLE 1 Results of the fits to $M(\pi\pi)$ of fig. 4 for ρ-production.

Reaction	mass m_o (MeV)	width Γ_o (MeV)	χ^2/ND	cross section (μb)
(A) $pp \to pp\pi^+\pi^-$	770	150	23/25	150 ± 21
(B) $pn \to pp\pi^-\pi^0$	770	180	33/29	139 ± 19
(C) $pn \to p_F n_B \pi^+\pi^-$	770	150	24/25	100 ± 24
(D) $pn \to p_B n_F \pi^+\pi^-$	770	150	33/29	92 ± 20

TABLE 2 Results of the fits to $M(\pi^+\pi^-)$ of fig. 7 for f^0-production.
The cross sections are corrected for unobserved decay modes.

Reaction	mass m_o (MeV)	width Γ_o (MeV)	χ_2/ND	cross section (μb)
(A) $pp \to pp\pi^+\pi^-$	1270	200	43/30	61 ± 20
(C) $pn \to p_F n_B \pi^+\pi^-$	1270	200	26/30	84 ± 38
(D) $pn \to p_B n_F \pi^+\pi^-$	1270	200	30/30	36 ± 16

TABLE 3 Cross sections in μb for single ρ production.

Reaction	p_{lab} (GeV/c)	4.0	5.0	5.5	6.0	6.6	6.9	7.0	8.0	10.	12.0	13.1	16.0	19.1	21.8	24.0	24.8
	refs	12	13[b)]	14	15[b)]	16	17	18	19[b)]	20[b)]	8	21	22[f)]	this exp.	23[b)]	8	24[b)]
σ_1 $p_1p_2 \rightarrow p_3(p_4\rho^o)$		55[a)] $\pm$15	70[a)] $\pm$20	35 $\pm$25	70[a)] $\pm$25	49 $\pm$10	65 $\pm$20		100[a)] $\pm$20	114 $\pm$19	96 $\pm$14	80[d)] $\pm$15		75 $\pm$10	64[c)] $\pm$15	63 $\pm$10	62[c)] $\pm$15
σ_2 $p_1n_2 \rightarrow p_3(p_4\rho^-)$														36 $\pm$17			
σ_3 $p_1n_2 \rightarrow (p_3\rho^-)p_4$														53 $\pm$10			
σ_4 $p_1n_2 \rightarrow p_3(n_4\rho^o)$								< 11						50 $\pm$12			
σ_5 $p_1n_2 \rightarrow (n_3\rho^o)p_4$								50 $\pm$ 15						46 $\pm$10			
$\sigma_2 + \sigma_3$								70[e)] $\pm$ 40									

a) Obtained from the World Collaboration DST [11], as events above handdrawn background after applying the mass cut described in section 3.2

b) No ρ^o-production claimed

c) Obtained from The World Collaboration DST [11], in the same way as at 19 GeV/c, see section 3.2.

d) Ref. [21] reports (70 $\pm$ 20) μb. (160 $\pm$ 30) μb is obtained as events above hand drawn background in the $(\pi^+\pi^-)$-mass plot of ref. [21].

e) Ref. [18] reports (25 - 70) μb for $|t_N| \leq 0.5$ $(GeV/c)^2$; t_N = momentum transfer to any of the nucleons. (70 $\pm$ 40) μb is estimated by us.

f) Reports evidence for some ρ^o production in $pp \rightarrow pp\pi^+\pi^-$, but no cross section given.

TABLE 4   Cross sections in μb for single f^o production. The cross sections are corrected for unobserved decay modes

Reaction	p_{lab} (GeV/c)	6.0	6.6	6.92	8.0	10.0	12.0	19.1	21.8	24.0	24.8
	refs	15	16	18	19	20	[illegible]	this exp.	23	[illegible]	24
σ_1	$p_1p_2 \to p_1(p_2f^o)$	$40^{a)}$ ± 15	28 ± 12	$65^{a)}$ ± 25	$90^{a)}$ ± 30	58 ± 25	39 ± 12	31 ± 10	$35^{a)}$ ± 20	70 ± 10	$32^{a)}$ ± 19
σ_2	$p_1n_2 \to p_1(n_2f^o)$							42 ± 19			
σ_3	$p_1n_2 \to (n_1f^o)p_2$							18 ± 8			

a) **Obtained from the World Collaboration DST [11], as events above handdrawn background after applying the mass cut described in section 3.2.**

TABLE 5 Intervals of the isospin cross sections and of the interference terms (in μb) for single ρ production at 19 GeV/c in the single and double exchange representations.

Single exchange		Double exchange	
m_0	(178 + 24) - (36 - 17)	m^{01}	(178 + 24) - (36 - 13)
m_1	(221 + 27) - (80 - 30)	m^{10}	(10 + 6) - (151 - 23)
m_3	(8 - 8) - (297 + 56)	m^{11}	207 $\pm$ 50
m_{01}	(-106-32) - (41 + 11)	$m^{01,10}$	19 $\pm$ 11
m_{03}	(22 + 20) - (-49 - 14)	$m^{01,11}$	(-100 - 38) - (73 + 11)
m_{13}	(-41 - 23) - (30 + 20)	$m^{10,11}$	(- 45 - 10) - (129 - 34)
β_{01}	(-.52-.13)- (.77 + .13)	$\beta^{01,10}$	(0.46 + 0.32) - (0.25 - 0.17)
β_{03}	(.61+.40) - (-.47-.18)	$\beta^{1,11}$	(0.52 - 0.15) - (0.85 + 0.14)
β_{13}	(-.99-.07) - (.20+.15)	$\beta^{10,11}$	(-0.99 - 0.04) - (0.73 + 0.11)

TABLE 6 Isospin cross section terms (in μb) and the normalized interference term ε for single f^o production at 19 GeV/c. For notation, see text.

Cross sections		
m_0	$= m^{00}$	32 ± 11
m_1	$= \frac{1}{3} m^{11}$	41 ± 18
m_{01}	$= \frac{1}{\sqrt{3}} m^{00,11}$	8 ± 16
β_{01}	$= \beta^{00,11}$	0.23 ± 0.45
F_0	$= F^{00}$	64 ± 22
F_1	$= F^{11}$	27 ± 12

TABLE 7 Results of the fit $m^{ij} = k_{ij}\, p_{lab}^{n_{ij}}$, $\beta_{ij,k\ell}$ = constant, to all ρ production cross sections modified for phase space effects, in the double peripheral representation. k_{ij} are the cross sections at p_{lab} = 1 GeV/c in mb.

$\chi^2/ND = 16.7/11$	
n_{01}	-0.40 ± 0.20
n_{10}	-1.0 ± 0.1
n_{11}	-0.82 ± 0.30
k_{01}	0.38 ± 0.20
k_{10}	4.0 ± 2.0
k_{11}	4.6 ± 4.0
$\beta_{01,10}$	0.3 ± 0.1
$\beta_{01,11}$	0.03 ± 0.2
$\beta_{10,11}$	0.6 ± 0.2

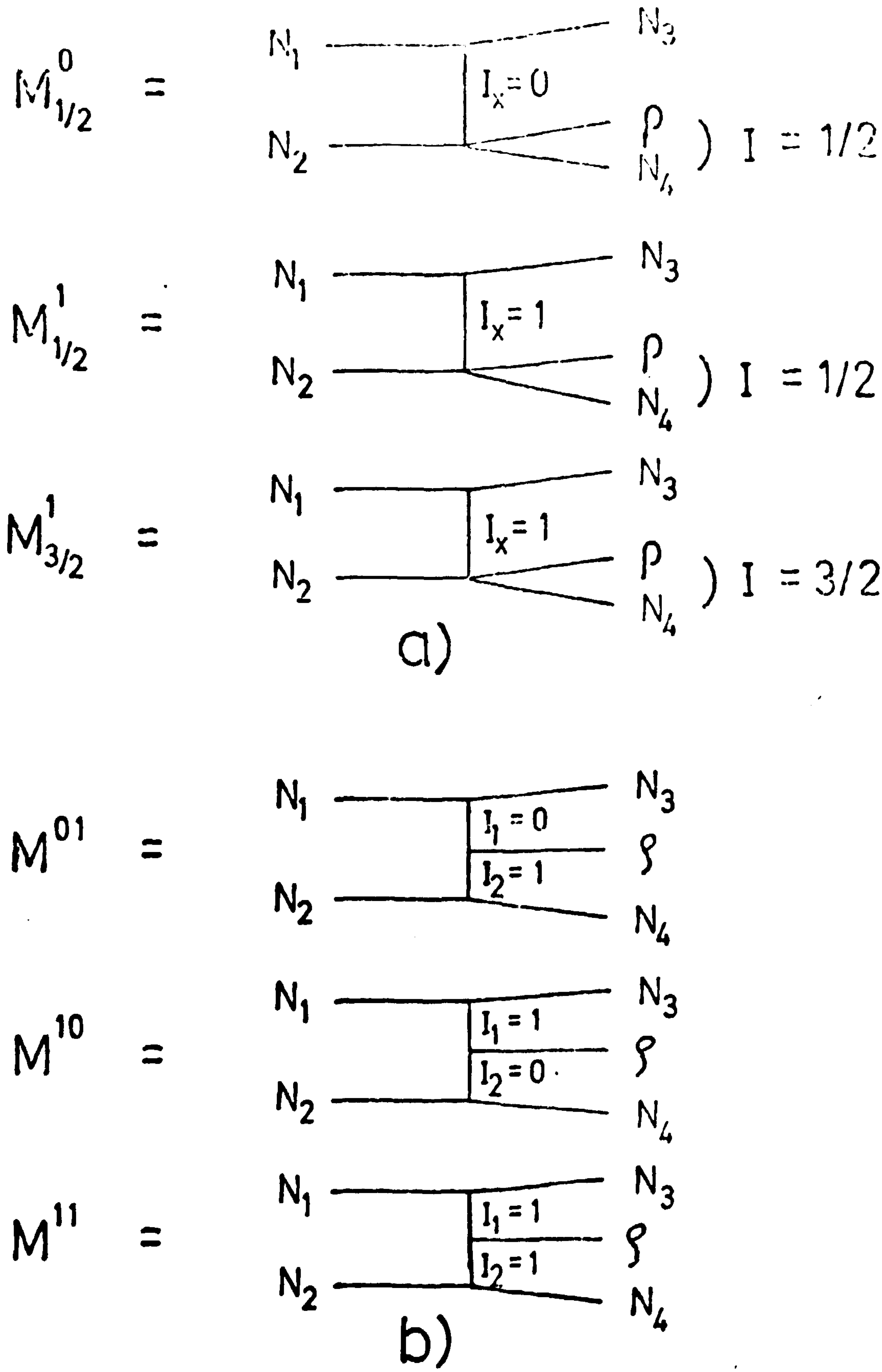

$M^0_{1/2}$ =
N_1
N_2
N_3
$I_x = 0$
ρ
N_4
) I = 1/2
$M^1_{1/2}$ =
N_1
N_2
N_3
$I_x = 1$
ρ
N_4
) I = 1/2
$M^1_{3/2}$ =
N_1
N_2
N_3
$I_x = 1$
ρ
N_4
) I = 3/2
a)
M^{01} =
N_1
N_2
$I_1 = 0$
$I_2 = 1$
N_3
ρ
N_4
M^{10} =
N_1
N_2
$I_1 = 1$
$I_2 = 0$
N_3
ρ
N_4
M^{11} =
N_1
N_2
$I_1 = 1$
$I_2 = 1$
N_3
ρ
N_4
b)

Fig. 1

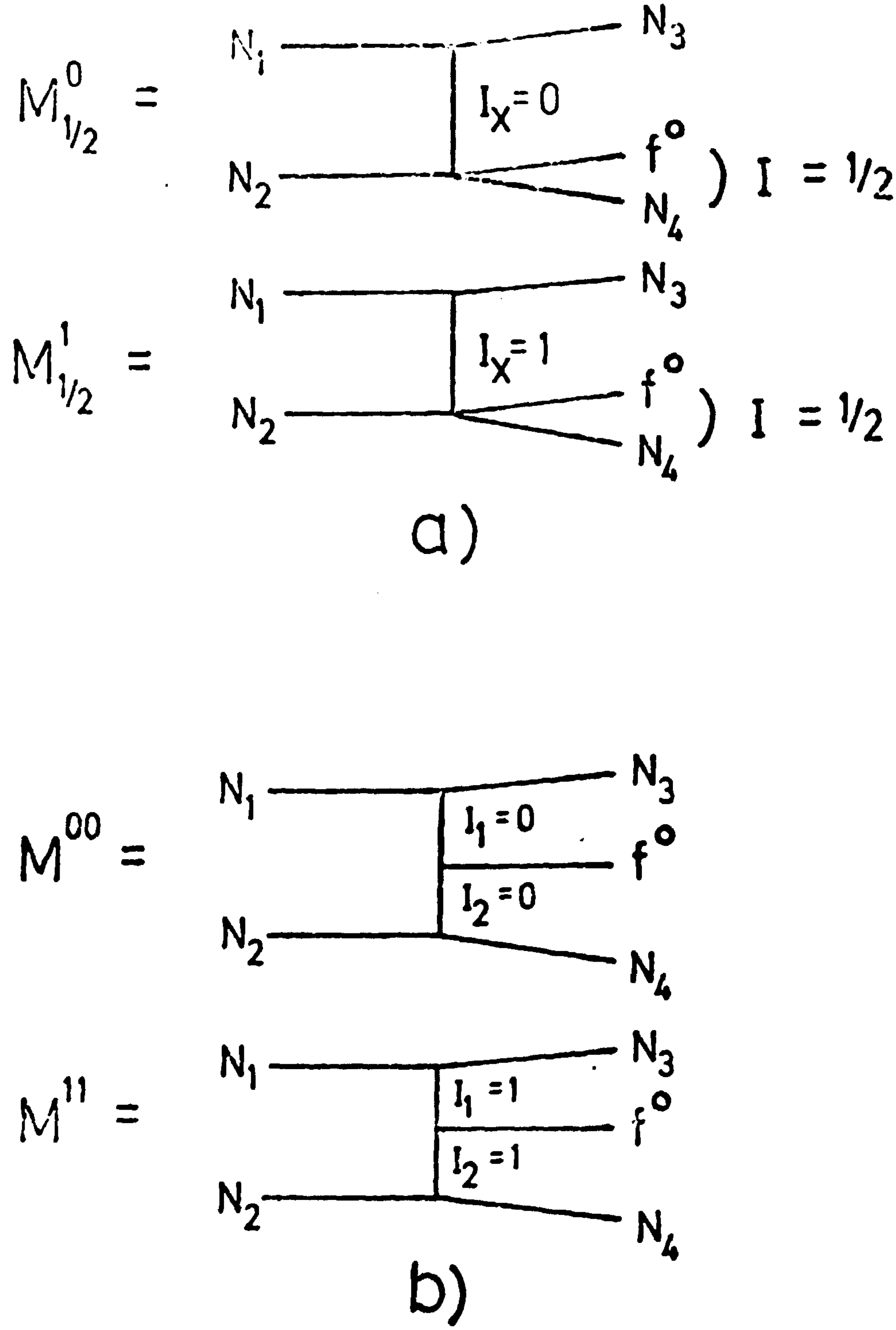

M$^0_{1/2}$ =
N$_1$
N$_3$
I$_X$= 0
N$_2$
f°
N$_4$
) I = 1/2
M$^1_{1/2}$ =
N$_1$
N$_3$
I$_X$= 1
N$_2$
f°
N$_4$
) I = 1/2
a)
M^{00} =
N$_1$
N$_3$
I$_1$ = 0
f°
I$_2$ = 0
N$_2$
N$_4$
M^{11} =
N$_1$
N$_3$
I$_1$ = 1
f°
I$_2$ = 1
N$_2$
N$_4$
b)

Fig. 2

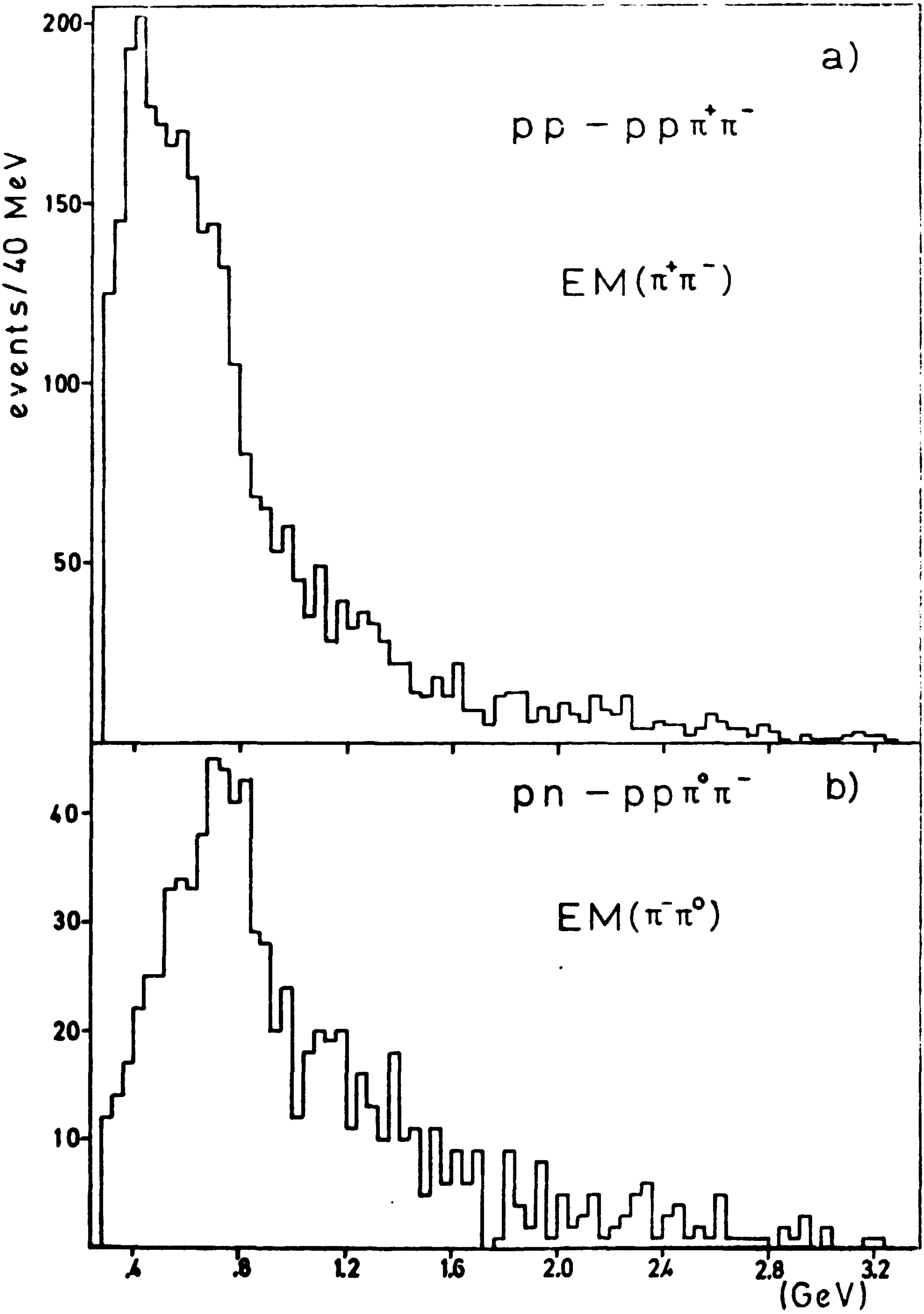

a)
pp – ppπ⁺π⁻
EM(π⁺π⁻)
events/40 MeV
200
150
100
50
b)
pn – ppπ°π⁻
EM(π⁻π°)
40
30
20
10
.4
.8
1.2
1.6
2.0
2.4
2.8
3.2
(GeV)

Fig. 3 a, b

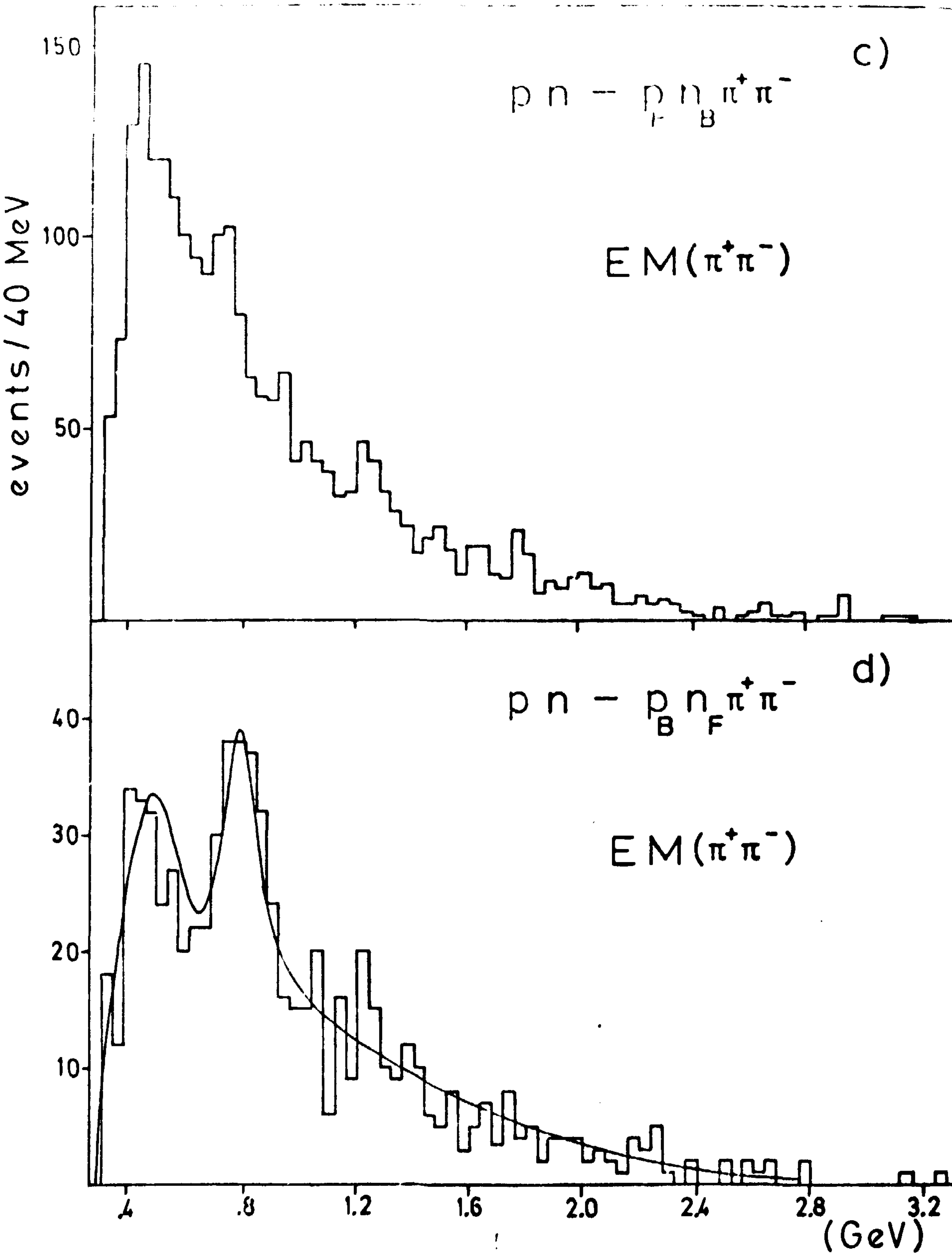
c)
p n − p_F n_B π⁺π⁻
EM(π⁺π⁻)
events / 40 MeV
150
100
50
d)
p n − p_B n_F π⁺π⁻
EM(π⁺π⁻)
40
30
20
10
.4
.8
1.2
1.6
2.0
2.4
2.8
3.2
(GeV)

Fig. 3 c, d

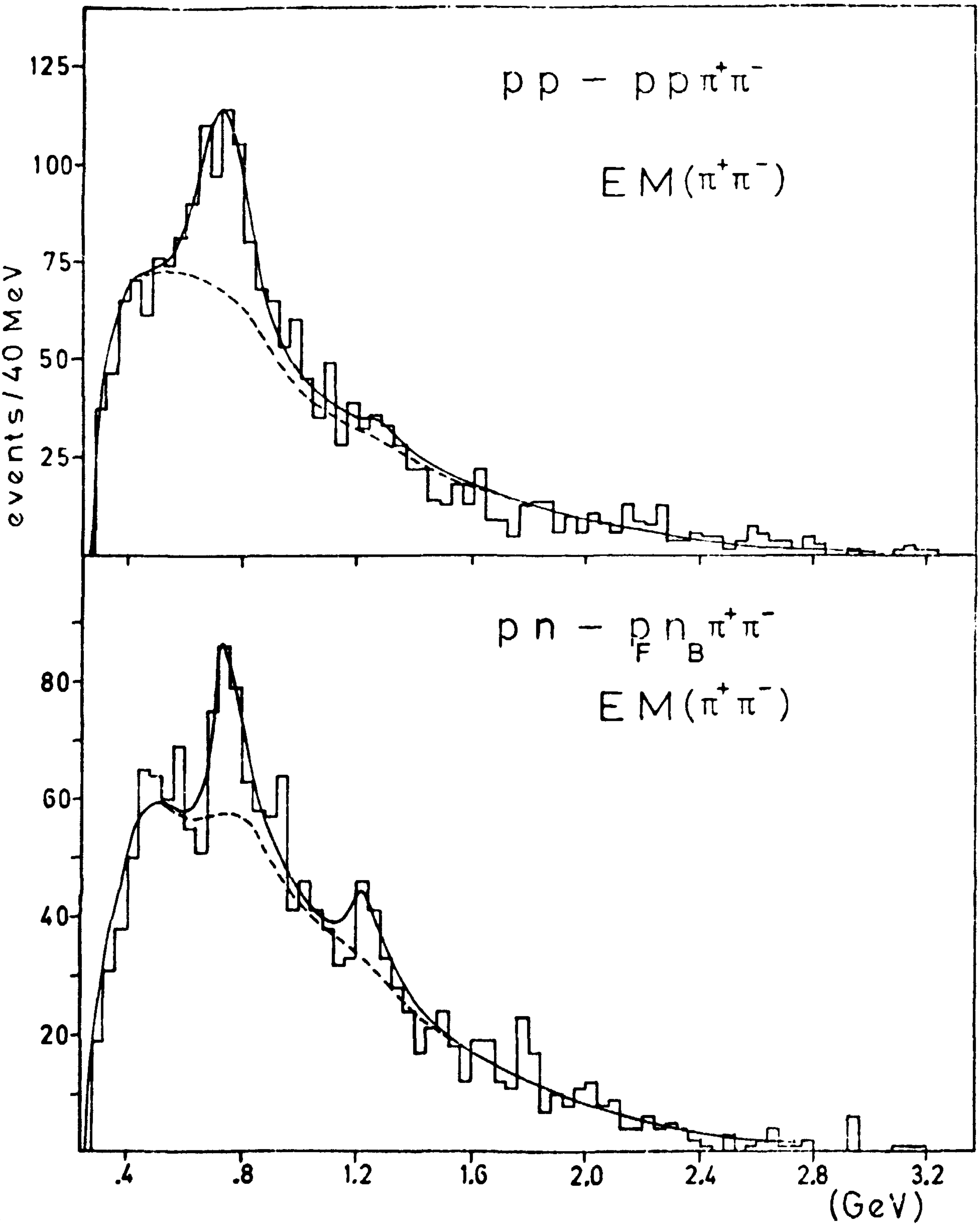
p p − p p π⁺π⁻
EM(π⁺π⁻)
p n − p_F n_B π⁺π⁻
EM(π⁺π⁻)
events/40 MeV
125
100
75
50
25
80
60
40
20
.4
.8
1.2
1.6
2.0
2.4
2.8
3.2
(GeV)

Fig. 4 a, b

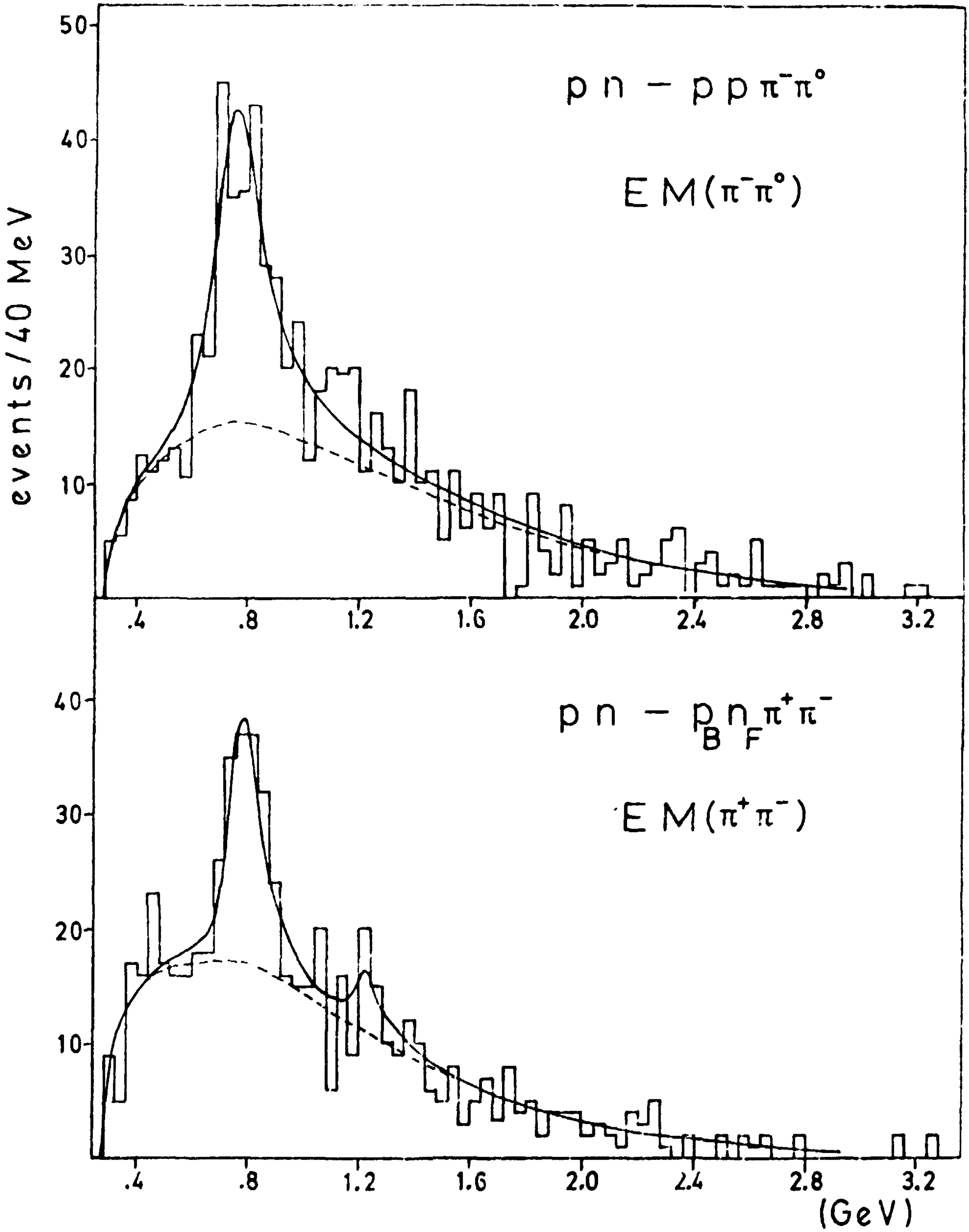

Fig. 4 c, d

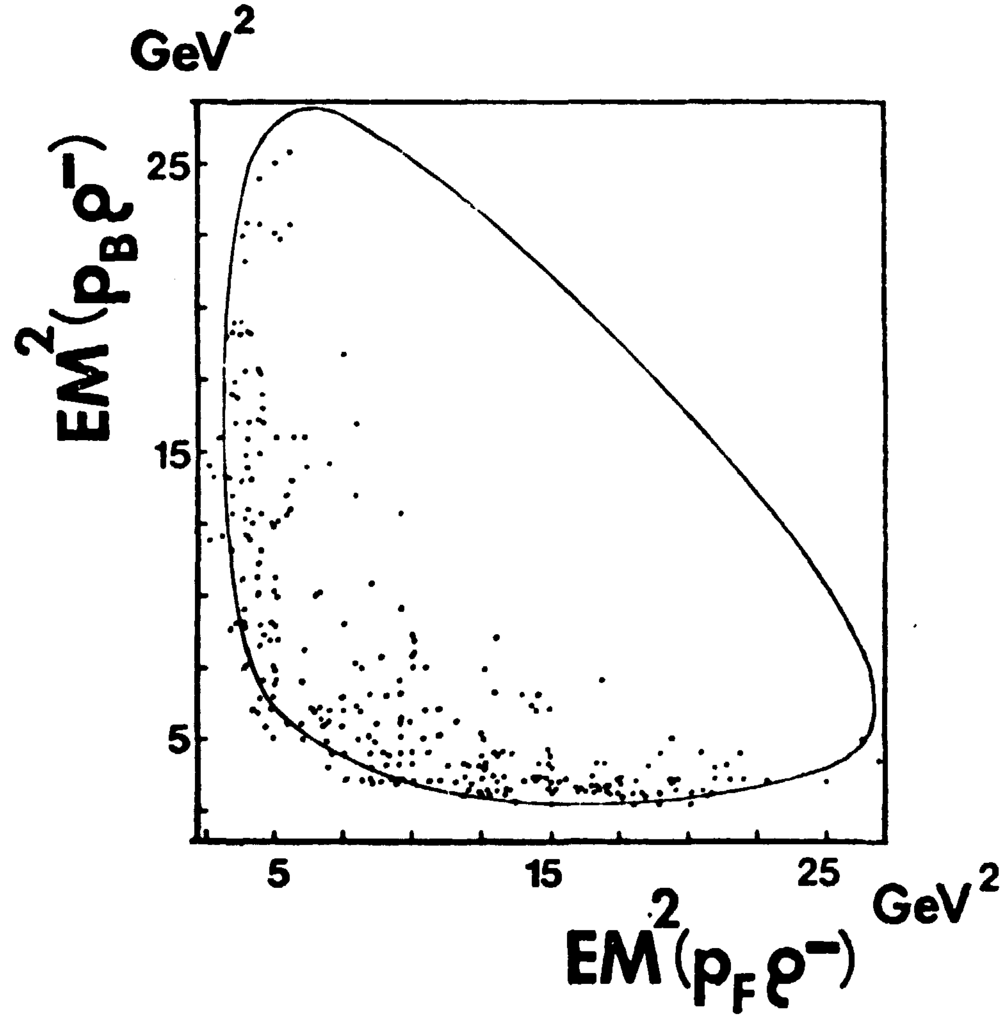

Fig. 5

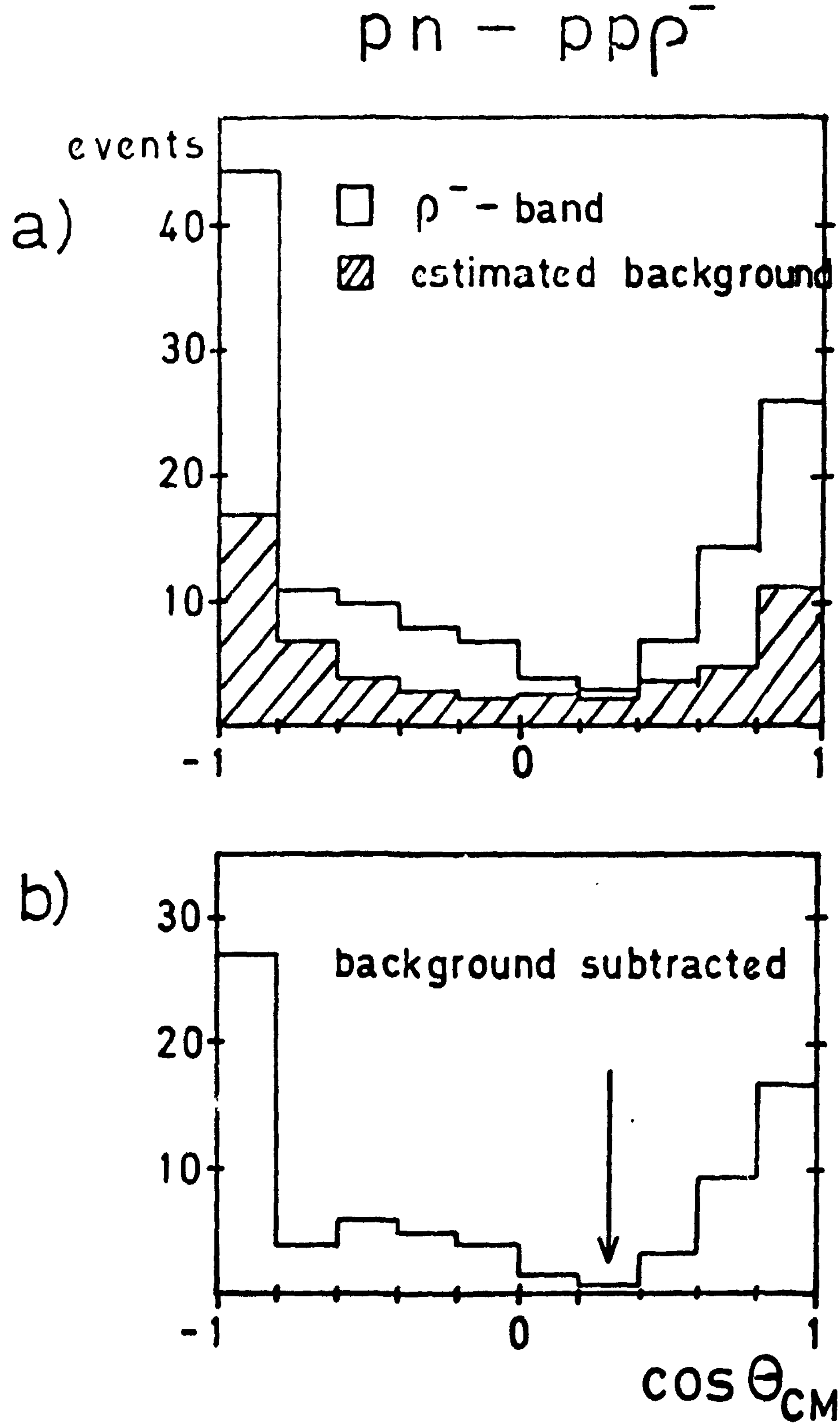

pn – ppρ⁻
events
a)
40
30
20
10
-1
0
1
ρ⁻ - band
estimated background
b)
30
20
10
-1
0
1
background subtracted
cos Θ_CM

Fig. 6

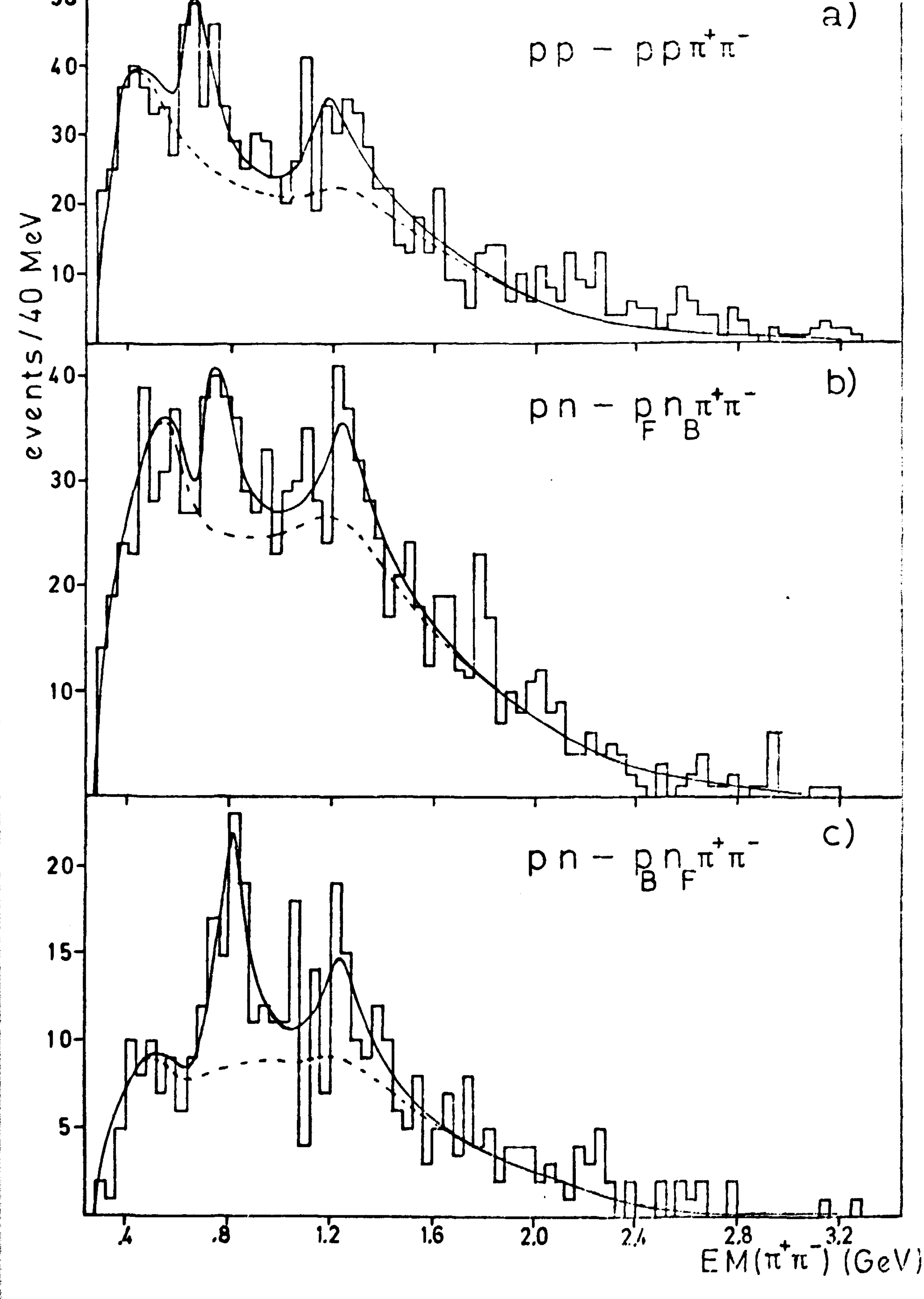
a)
pp – ppπ⁺π⁻
b)
pn – p_F n_B π⁺π⁻
c)
pn – p_B n_F π⁺π⁻
events / 40 MeV
EM(π⁺π⁻) (GeV)
.4
.8
1.2
1.6
2.0
2.4
2.8
3.2

Fig. 7

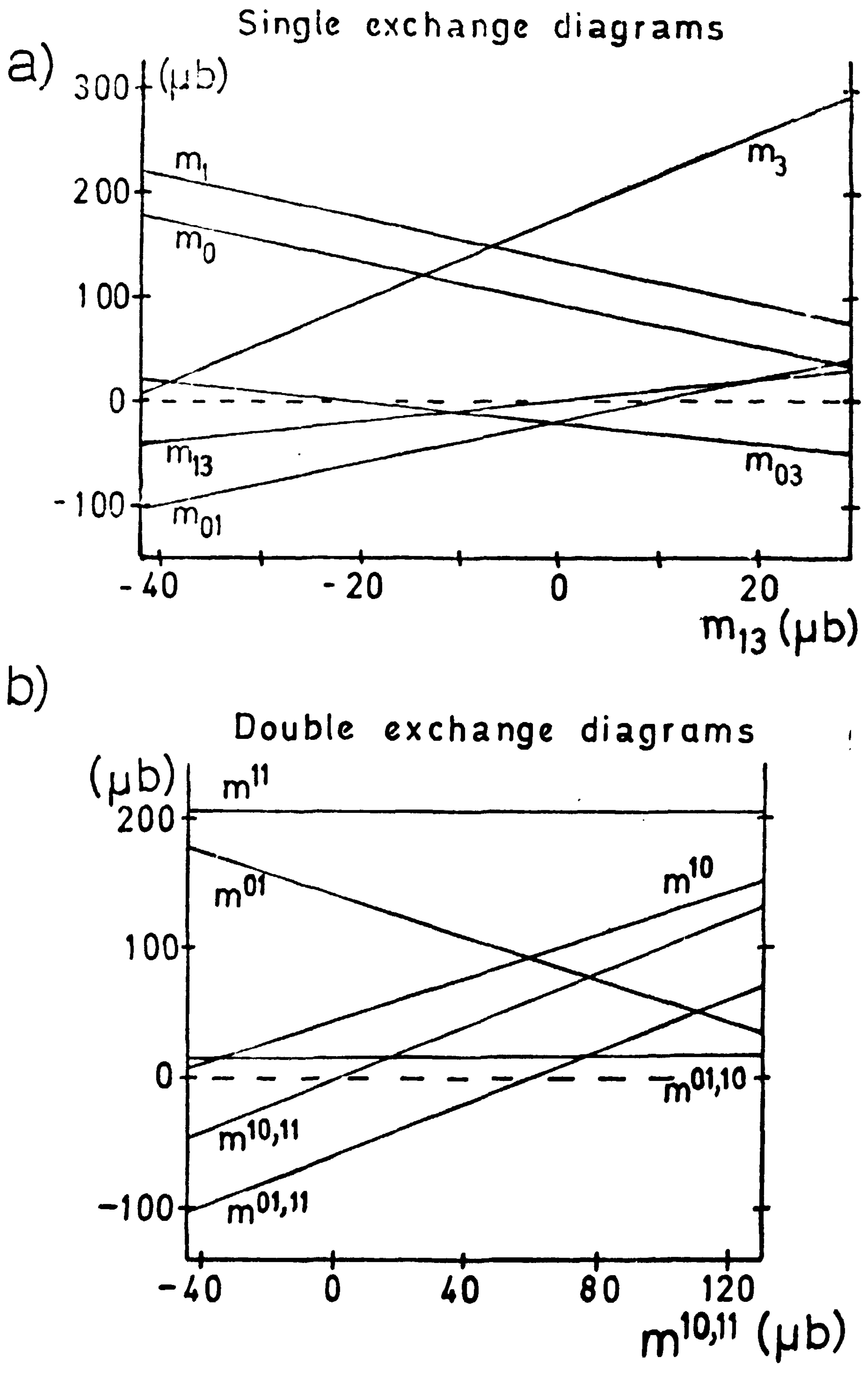

Single exchange diagrams
a)
(μb)
300
200
100
0
-100
m_1
m_0
m_3
m_{13}
m_{03}
m_{01}
-40
-20
0
20
m_{13} (μb)
b)
Double exchange diagrams
(μb)
200
100
0
-100
m^{11}
m^{01}
m^{10}
$m^{01,10}$
$m^{10,11}$
$m^{01,11}$
-40
0
40
80
120
$m^{10,11}$ (μb)

Fig. 8

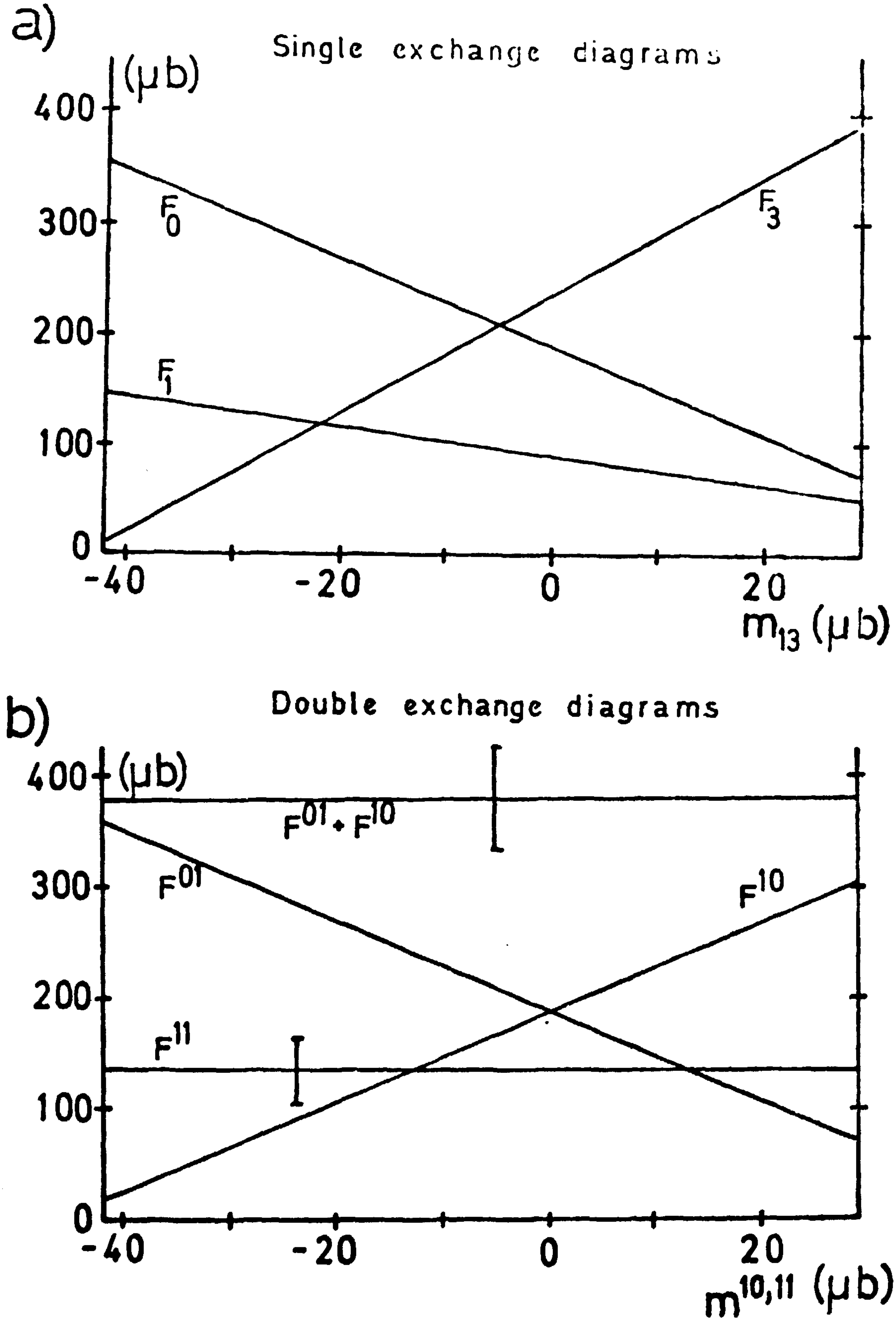
a)
Single exchange diagrams
(μb)
400
300
200
100
0
F_0
F_1
F_3
-40
-20
0
20
m_{13} (μb)
b)
Double exchange diagrams
(μb)
400
300
200
100
0
$F^{01}+F^{10}$
F^{01}
F^{10}
F^{11}
-40
-20
0
20
$m^{10,11}$ (μb)

Fig. 9

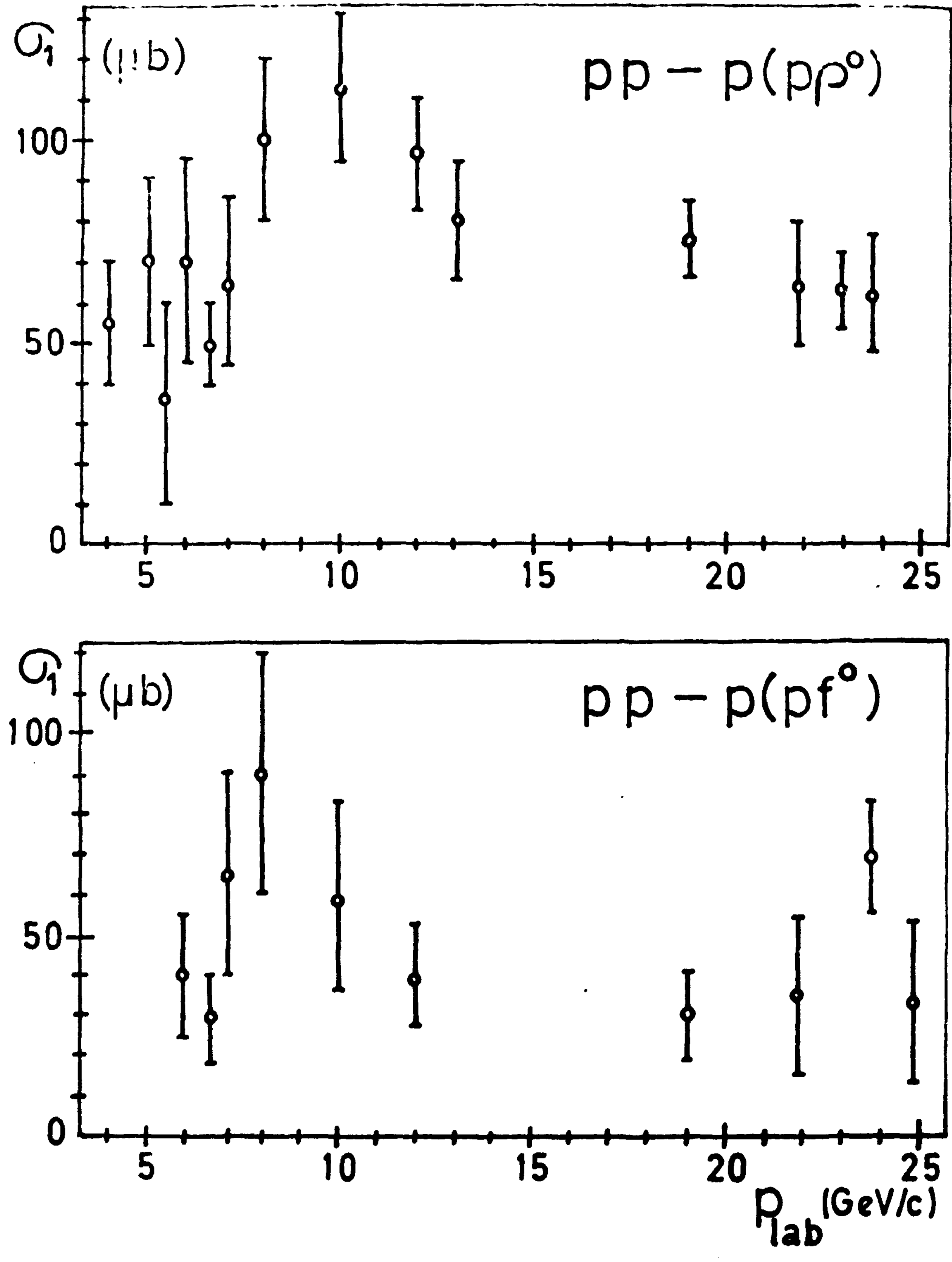

σ_1 (μb)
pp − p(pρ°)
100
50
0
5
10
15
20
25
σ_1 (μb)
pp − p(pf°)
100
50
0
5
10
15
20
25
p_{lab} (GeV/c)

Fig. 10

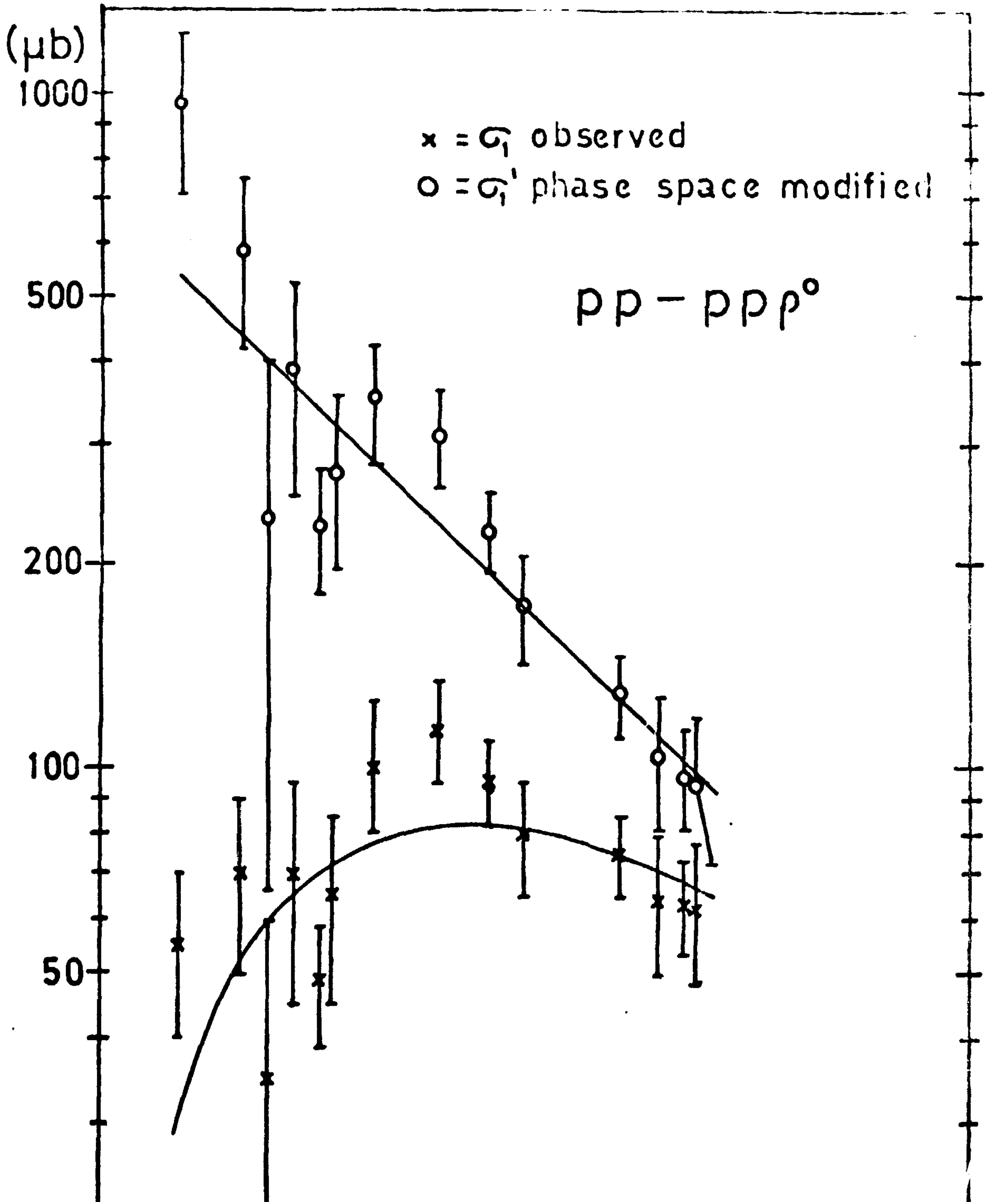

(μb)
1000
500
200
100
50
20
x = σ_1 observed
o = σ_1' phase space modified
pp − ppρ°
3
5
10
20
30
p_{lab} (GeV/c)

Fig. 11

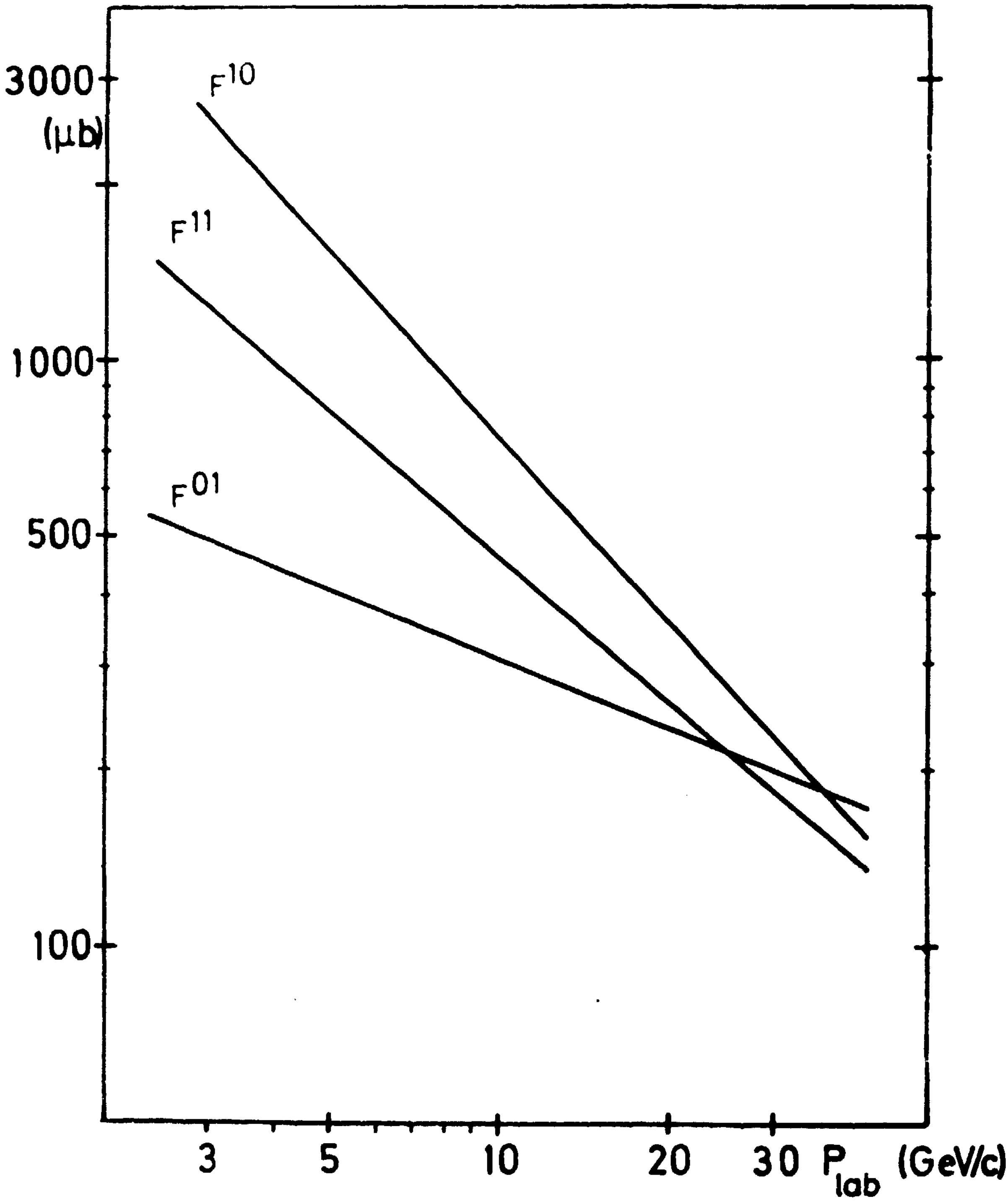

Fig. 12